THE IMPROVEMENT IN SEPARATION OF CONCENTRIC TUBE THERMAL DIFFUSION COLUMNS

A THESIS

Presented to

The Faculty of the Graduate Division

by

Ho-Ming Yeh

In Partial Fulfillment

of the Requirements for the Degree

Doctor of Philosophy in the School of Chemical Engineering

Georgia Institute of Technology

June, 1969

In presenting the dissertation as a partial fulfillment of the requirements for an advanced degree from the Georgia Institute of Technology, I agree that the Library of the Institute shall make it available for inspection and circulation in accordance with its regulations governing materials of this type. I agree that permission to copy from, or to publish from, this dissertation may be granted by the professor under whose direction it was written, or, in his absence, by the Dean of the Graduate Division when such copying or publication is solely for scholarly purposes and does not involve potential financial gain. It is understood that any copying from, or publication of, this dissertation which involves potential financial gain will not be allowed without written permission.

_____

7/25/68

THE IMPROVEMENT IN SEPARATION OF
CONCENTRIC TUBE THERMAL DIFFUSION COLUMNS

Approved:

Chairman

Date approved by Chairman: 5/28/69

ACKNOWLEDGMENTS

The author is grateful to his thesis advisor, Dr. Henderson C. Ward, for his interest and helpful suggestions during this study. The constructive criticisms given by Dr. Homer V. Grubb and Dr. Charles W. Gorton, in their reading of this work are acknowledged with thanks.

In the construction and setting up of the experimental equipment used in this study, the help of Mr. C. A. Mayes and Mr. C. Blackwood was invaluable.

The author also expresses his appreciation to the Chinese National Science Council for providing a fellowship for study at the Georgia Institute of Technology.

Finally, the author is grateful for the encouragement and understanding shown by his wife.

TABLE OF CONTENTS

TABLE OF CONTENTS (Continued)

LIST OF TABLES

LIST OF FIGURES

LIST OF FIGURES (Continued)

NOMENCLATURE

This table contains symbols which are used frequently throughout this work. It does not include common mathematical symbols or symbols which are defined and used only locally within the body of the work.

Symbol	Definition
A	system constant evaluated by Equation (9)
B	column width of parallel plate column or wire spacing of wired concentric tube column
c	fractional mass concentration of component 1 in a binary solution
$\bar{c}$	fractional mass concentration of component 2, 1-c
c_{fe}	fractional mass concentration of component 1 in the product stream exiting from the enriching section
c_{fs}	fractional mass concentration of component 1 in the product stream exiting from the stripping section
$c_o(o,z)$	fractional mass concentration of component 1 at x = 0
D	ordinary diffusion coefficient
g	gravitational acceleration
H	system constant evaluated by Equation (22)
H_o	system constant evaluated by Equation (44)
h	height of concentric tube column
J_x	mass flux of component 1 in x-direction

$J_{x\text{-}TD}$	mass flux of component 1 in x-direction due to thermal diffusion
$J_{z\text{-}OD}$	mass flux of component 1 in z-direction due to ordinary diffusion
K_c	system constant
K_{ce}	K_c for enriching section evaluated by Equation (24)
K_d	system constant evaluated by Equation (25)
K_e	$K_{ce} + K_d$
K_o	system constant evaluated by Equation(45)
K_s	$K_e \mid \sigma_e \rightarrow \sigma_s$
L	length of parallel plate column
p	pressure
R_1	outside radius of inner tube of concentric tube column
R_2	inside radius of outer tube of concentric tube column
T	absolute temperature
T_m	arithetric mean temperature of hot and cold surfaces
$\overline{T}$	reference temperature
T_1	temperature of cold wall
T_2	temperature of hot wall
ΔT	$T_2 - T_1$
$v_z(x)$	general velocity distribution function of fluid flowing in z-direction

ν_z'	$\dfrac{12\mu\ \nu_z}{\overline{\beta}_T\ \omega^2(\Delta T)g\ \cos\ \phi}$
x	axis normal to the surface
z	axis parallel to the surfaces in parallel plate columns, or axis parallel to the wire in concentric tube columns
z_{fe}	length of the enriching section measured along z-axis
z_{fs}	length of the stripping section measured along z-axis
α	thermal diffusion constant
$\overline{\beta}_T$	$-\left(\dfrac{\partial\rho}{\partial T}\right)_p$ measured at $\overline{T}$
γ	a constant defined by Equation (13)
Δ	difference in concentration of top and bottom products
Δ'	reduced separation, $\dfrac{\Delta\sigma}{H_o}$
Δ_{max}	Δ when $\phi = \phi_{opt}$
Δ'_{max}	Δ' when $\phi = \phi_{opt}$
Δ_o	Δ obtained in open column
η	$\dfrac{x}{\omega}$
μ	absolute viscosity
ϕ	wire angle of inclination from the vertical
ϕ_{opt}	optimum wire angle of inclination for maximum separation
ρ	mass density

$\bar{\rho}$	ρ measured at $\bar{T}$
σ	mass flow rate
σ'	reduced mass flow rate, $\frac{\sigma h}{K_o}$
σ_e	mass flow rate in the enriching section
σ_s	mass flow rate in the stripping section
τ_1	transport of component 1 along z-direction
$\Psi(z)$	relation defined by Equation (13)
ω	one-half of the distance between hot and cold walls

SUMMARY

The convective currents produced by the temperature gradient in a thermal diffusion column have two conflicting effects: the desirable cascading effect which is necessary in securing high separation, and the undesirable remixing effect. It appears, therefore, that proper control of the convective strength might effectively suppress this undesirable remixing effect while still preserving the desirable cascading effect, and thereby lead to improved separation.

The improvement in the degree of separation of a concentric tube thermal diffusion column by means of a wire spiral, having a diameter equal to the annular spacing and inserted as a spacer in the annular region, was investigated. It was shown that the undesirable remixing effect could be effectively reduced and controlled by this type of wire and a substantial improvement in separation efficiency attained.

The most important assumptions in this work are that the concentration in the column is anywhere between 0.3 to 0.7 weight fraction, and that the annular spacing is small compared with the tube diameters, which is generally true in a thermal diffusion column, and therefore that the effect of curvature of the wire spiral could be neglected. Based on these assumptions, a generalized equation of separation was derived. It was also found from theoretical consideration that an optimum wire angle of inclination and maximum separation exist for each moderately low flow rate. Equations for optimum wire angle of inclination and maximum separation were derived and graphically presented in

terms of dimensionless groups. No optimum wire angle of inclination exists when the flow rate exceeds a certain critical value and this critical value was evaluated. For flow rates above the critical value, insertion of a wire spiral will have the reverse effect of decreasing the separation.

Experimental runs with the systems benzene-n-heptane and toluene-isobutyl alcohol were made at various flow rates and wire angles of inclination, and the agreement with theory was good. The separation does go through a maximum, and the optimum wire angles were found to agree with theory. Experimental data also showed that no optimum wire angle of inclination and maximum separation exist when the flow rate exceeds the critical value, in accordance with theory.

Considerable improvement in separation was obtained by employing the wired column operating at the optimum wire angle of inclination instead of using the open column (the column without the wire spiral). This is particularly true for moderately low flow rates, and in one case the separation obtained in the wired column operating at the optimum wire angle of inclination exceeded that obtained in the open column by more than 150 percent.

CHAPTER I

INTRODUCTION

If two gases of different composition and initially at the same temperature are allowed to diffuse together, a transient temperature gradient results from the ordinary diffusion process. This phenomenon was first noted by Dufour[8]. Conversely, if a temperature gradient is applied to a homogeneous solution, a concentration gradient is usually established. The name thermal diffusion is generally applied to this second effect. The phenomenon of thermal diffusion was first discovered by Enskog[7] in 1911 from theoretical considerations of the kinetic theory of a mixture of gases and was later demonstrated experimentally by Chapman and Dootson[1] in 1917. Thus, a temperature gradient in a mixture of two gases or liquids gives rise to concentration gradients with one component concentrated near the hot wall and the other component concentrated near the cold wall. For molecules such that the interaction force between the molecules varies as an inverse power of the distance between the molecules, the direction of diffusion for powers greater than five is such that the lighter molecules in general move toward the warmer part of the solution, while for powers less than five, the lighter molecules accumulate in the colder part of the solution.

In static systems, which were used in the early work of thermal diffusion, the temperature gradient was applied in the vertical direction and there was no convection or bulk flow. The concentration gradient at

steady-state was such that the flux due to ordinary diffusion just counterbalanced that resulting from thermal diffusion. The steady-state separation obtainable from such a single, static stage was generally so slight that it was of theoretical interest only. It was the great achievement of Clusius and Dickel[3,4] to point out that convective currents could be utilized to produce a cascading effect analogous to the multistage effect of countercurrent extraction and thus obtain a relatively large separation. A column utilizing these effects is called a Clusius-Dickel Column and consists essentially of two opposing vertical plates separated by a very narrow open space. One plate is heated and the other cooled, and the thermal diffusion effect causes one component of, say, a binary mixture to diffuse toward the hot plate. At the same time the density gradient which arises because of the temperature gradient causes smooth laminar convection currents up the hot plate and down the cold plate. Because of the concentration gradient set up by the thermal diffusion, the convection currents transport one component preferentially toward the top and thus create large concentration differences between the top and the bottom of the column. An excellent treatment of column theory applicable to moderate flow rates in parallel plate columns is given by Jones, Furry, and Onsager[9,10].

A more detailed study of the mechanism of separation in the Clusius-Dickel Column indicates that the convective currents actually have two conflicting effects: the desirable cascading effect, and the undesirable remixing effect. The convective currents have a multistage effect which is necessary in securing high separation, and it is an essential feature of the Clusius-Dickel Column. However, since the

convection currents bring down the fluid at the top of the column, where it is rich in one component, to the bottom of the column, where it is rich in the other component, and vice versa, there is a remixing of the two components. It appears, therefore, that proper control of the convective strength might effectively suppress this undesirable remixing effect while still preserving the desirable cascading effect, and thereby lead to improved separation.

One of the reports of improved separation of liquid mixtures resulting from modification of the convective flow pattern was made by Debye and Bueche[6]. They employed a batch-type column in which the annular spacing was packed with glass wool. Later, Powers and Wilke[11] demonstrated that the degree of separation in a continuous-type flat plate apparatus was improved when the convective flow was reduced by tilting the apparatus at various angles. The best angles of inclination for maximum separation were later investigated both theoretically and experimentally by Chueh and Yeh[2]. Experimental results for the benzene-n-heptane system were in excellent agreement with theory.

Sullivan, Ruppel, and Willingham[12] tested two batch-type columns in which the inner tube was rotated and a third batch-type column in which the annulus was packed with glass wool. For a given annular space, the packed column produced better separation than the rotated columns. Both rotary and packed columns gave better separations than an open column with the same annular spacing. In a more intensive study of batch-type packed thermal diffusion columns, Sullivan, Ruppel, and Willingham[13] found that improved separations were obtained in various wide-annular columns (0.03 to 0.125 inch) when the annular spacing was

packed with glass wood. They indicated that the degree of separation obtained at steady-state was a function of both the annular spacing and the packing density. For a fixed annular spacing, the degree of separation increased with packing density. However, the lowest packing density gave the fastest approach to steady-state.

The work reported by Washall and Melpolder[14] was an attempt to increase the separation efficiency of a batch-type liquid thermal diffusion column by winding a wire helix within the annulus of the column. Both the wire diameter and the wire angle of inclination were critical factors affecting the maximum separation attainable. Greatest separations were obtained when the diameter of the wire was essentially equal to the annular spacing.

It is the purpose of this work to investigate both theoretically and experimentally, the improvement in the degree of separation of a concentric tube thermal diffusion column operating under steady-state conditions by means of a wire spiral, having a diameter equal to the annular spacing and inserted as a spacer in the annular region.

It is not yet clear how thermal diffusion would stand in the economic picture when compared with conventional separation processes, as operating data are practically nonexistent. However, the process has been applied to the separation of highly valuable materials which are difficult or impossible to separate by other means.

CHAPTER II

COLUMN THEORY

Thermal Diffusion in a Flat Plate Column

The temperature gradient applied between the surfaces of a flat plate thermal diffusion column has two effects: (1) a flux of one component of the solution relative to the other is brought about by thermal diffusion, and (2) convective currents are produced parallel to the plates owing to density differences. The combined result of these two effects is to produce a concentration difference between the two ends of the column which is generally much greater than that obtained by the static method. Meanwhile, the concentration gradient produced by the combined effects of thermal diffusion and convection acts to oppose thermal diffusion and limits the separation. Figure 1 illustrates the flows and fluxes prevailing in a continuous flow column.

Thermal Diffusion in a Wired Concentric Tube Column

Now, we consider a concentric tube thermal diffusion column with a tight fitting wire spiral, having a diameter equal to the annular spacing, wrapped on the entire inner tube as shown in Figure 2(a). Because of the diminutive size of the annular spacing as compared with the tube diameters, the transport phenomenon of this construction can be considered as that of a curved pipe of rectangular cross-section of very large aspect ratio, $\lambda = \frac{B}{\omega}$, whose exis is curved in a helical form.

In 1952, Cuming[5] gave the approximate solution of the Navier-

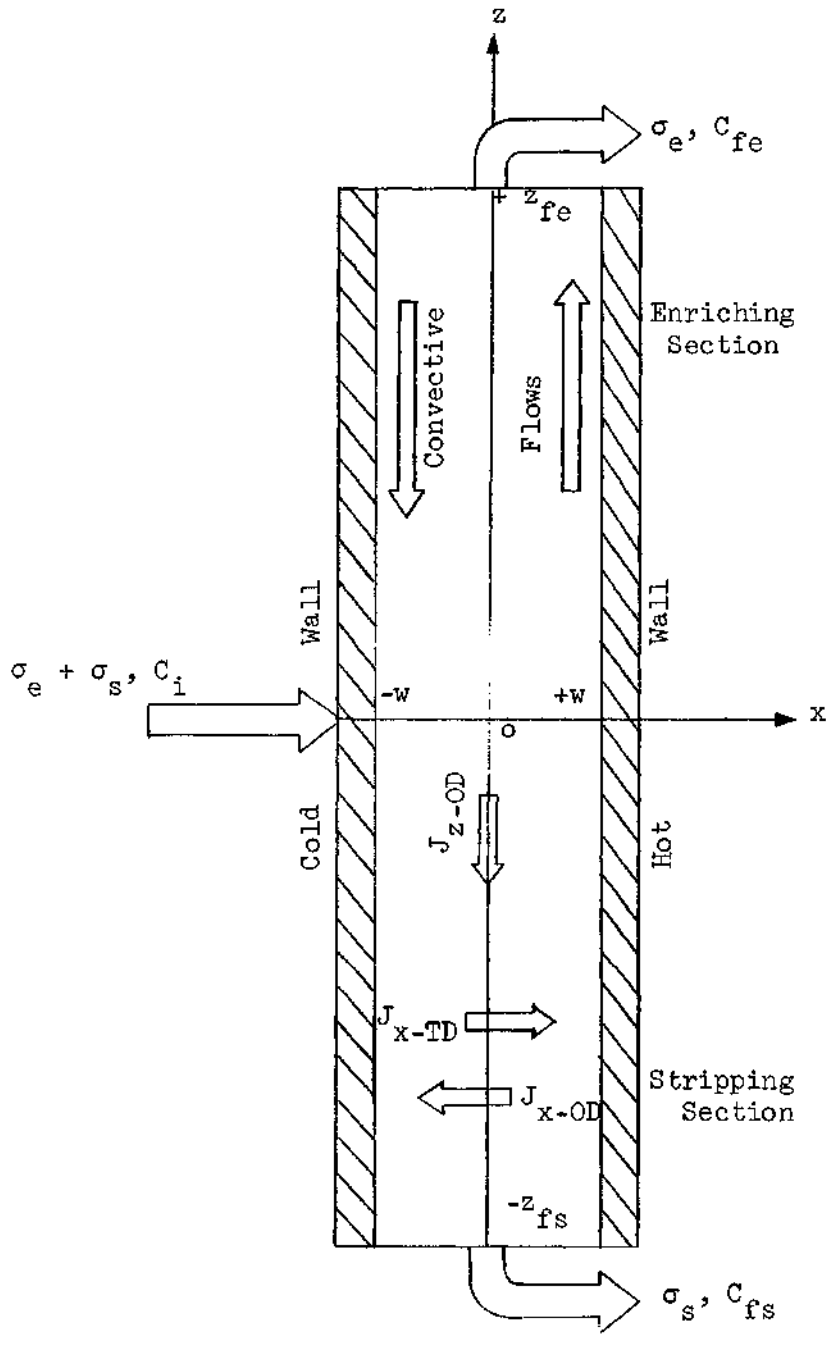

Figure 1. Schematic Diagram of a Continuous-Flow Thermal Diffusion Column

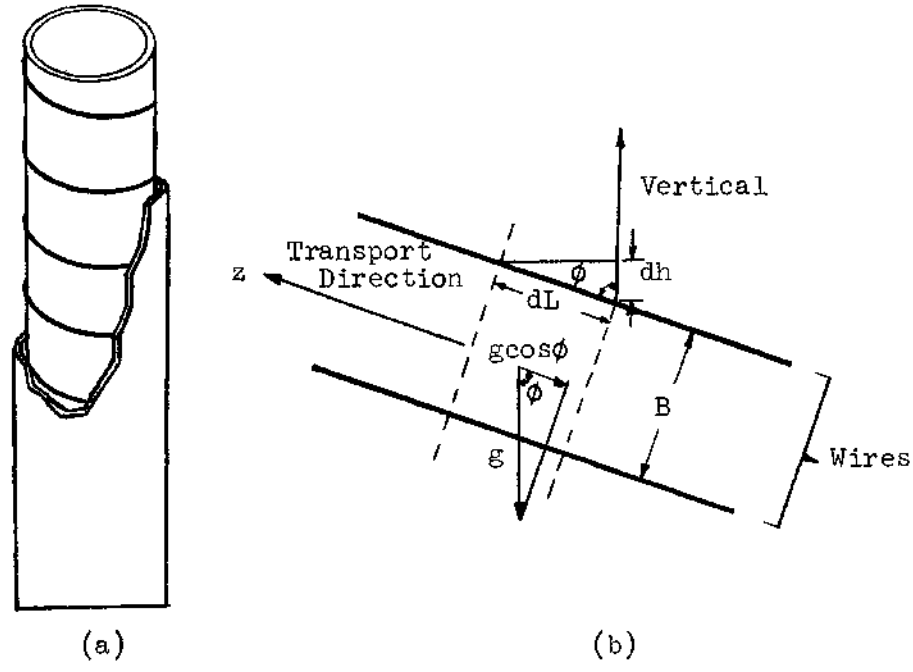

Figure 2. Spiral Wire Inserted as a Spacer in the Annulus of a Conventional Concentric Tube Thermal Diffusion Column

Stokes equation for the flow of a viscous incompressible fluid through a curved pipe of elliptical cross-section of very large aspect ratio and whose axis was curved in circular form, in a power series of the curvature of the pipe. He pointed out that the secondary flow vanishes altogether in this case and that the axial velocity distribution reduces to

$$v_o = \frac{Re}{2}(1-\eta^2)\left[1 - \frac{2\,k\omega}{3}\eta\right] \quad , \tag{1}$$

where v_o represents the non-dimensional axial velocity, Re the Reynolds number, and k the curvature of the pipe axis. Actually, the geometry of the ellipse approximates that of a rectangle when the aspect ratio is sufficiently large. Therefore, Equation (1) can be applied to a curved pipe of rectangular cross-section in the case of a sufficiently large aspect ratio. The absolute value of the second term in the bracket is very small compared with unity on account of the diminutive size of the annular spacing as compared with the tube diameters. Therefore, the velocity distribution reduces to

$$v_o = \frac{Re}{2}(1-\eta^2) \quad . \tag{2}$$

This is the same as the velocity distribution for flow between parallel plates. Thus, the effect of curvature can be neglected when the annular spacing is very small compared with the tube diameters in a wired concentric tube column.

For the wired column used in this study, which had an annular space of 0.0325 inch and an average annular region diameter of 1.3475 inch, $\left|\frac{2\,k\omega}{3}\eta\right| < |k\omega| < \left|\frac{\omega}{(R_1+R_2)/2}\right| = \frac{0.0325}{1.3475} = 0.024$. Therefore,

the effect of curvature is insignificant and this construction can be considered as a parallel flat plate column, inclined on edge, with rectangular cross-section of very large aspect ratio, as shown in Figure 2(b). In this case the gravitational force is divided and the strength of the convective currents produced by the temperature gradient is reduced under the influence of the wire spiral inserted in the annulus, and the transport direction z makes an angle ϕ from the vertical which is the angle of inclination of the wire spiral.

The derivation of the equation of separation proceeds in several steps. First, the convection velocity v_z is derived as a function of x. This result is used to obtain the horizontal mass flux J_x and the concentration distribution. Then the rate of mass transport τ in the z-direction is derived, and finally the equation of separation is obtained.

Velocity Distribution

Since the space between the plate surfaces of a thermal diffusion column is so small we may assume that the convective flow produced by the density gradient is laminar and that the temperature distribution is determined by conduction in the x-direction only. We also assume that the convection velocity is in the z-direction only, that both end effects can be neglected, and that the mass fluxes due to thermal and ordinary diffusion are too small to effect the velocity and temperature profiles. The hydrodynamical equation for steady laminar flow under the influence of gravity can be obtained by reducing the Navier-Stokes equation to

$$\mu \frac{d^2 v_z}{dx^2} = \frac{\partial p}{\partial z} + \rho g \cos \phi \quad . \tag{3}$$

Here the viscosity has been assumed to be constant.

Everywhere else in the calculation we shall identify ρ with $\bar{\rho}$, the density at temperature $\bar{T}$. Here, however, in order to calculate a non-vanishing value of v_z, we must use a better approximation for ρ. We now expand ρ in a Taylor series in T about some reference temperature $\bar{T}$ (as yet unspecified):

$$\rho = \rho\Big|_{\bar{T}} + \frac{\partial \rho}{\partial T}\Big|_{\bar{T}} (T-\bar{T}) \quad . \tag{4}$$

Furthermore, if the pressure gradient in the system is due solely to the weight of the fluid in the annulus, then $\frac{\partial p}{\partial z} = - \bar{\rho} g \cos \phi$ and the equation of motion, Equation (3), becomes

$$\frac{\mu}{\omega^2} \frac{d^2 v_z}{d\eta^2} = - \bar{\beta}_T g \cos \phi \, (T-\bar{T}) \quad , \tag{5}$$

in which $\eta = \frac{x}{\omega}$.

The approximation of constant thermal conductivity makes the temperature a linear function of x:

$$T = T_m + \frac{\Delta T}{2} \left(\frac{x}{\omega}\right) \quad , \tag{6}$$

in which $\Delta T = T_2 - T_1$ and $T_m = \frac{(T_1+T_2)}{2}$.

Substituting Equation (6) into Equation (5), we obtain

$$\frac{d^2 v_z}{d\eta^2} = - \frac{\bar{\beta}_T \omega^2 g \cos \phi}{\mu} \left[(T_m - \bar{T}) + \frac{\Delta T}{2} \eta \right] \quad . \tag{7}$$

Integrating Equation (7) and using the fact that v_z vanishes for $\eta = \pm 1$, we have

$$v_z = \frac{\bar{\beta}_T \omega^2 (\Delta T) g \cos \phi}{12 \mu} \left[(\eta - \eta^3) + A(1 - \eta^2) \right] \quad , \tag{8}$$

where

$$A = \frac{6(T_m - \bar{T})}{\Delta T} \quad .$$

To find the constant A, we make a material balance in the enriching section, giving

$$\sigma_e = \int_{-1}^{+1} \bar{\rho} \, v_z \, B \omega \, d\eta \quad . \tag{9}$$

Substitution of Equation (8) into this expression gives

$$A = \frac{6(T_m - \bar{T})}{\Delta T} = \frac{9 \sigma_e \mu}{\bar{\rho} \bar{\beta}_T B \omega^3 (\Delta T) g \cos \phi} \quad . \tag{10}$$

Equations (8) and (10) represent the steady velocity distribution of fluid flowing in the enriching section of a wired concentric tube thermal diffusion column in the direction parallel to the wires under continuous operation, while replacing σ_e with $-\sigma_s$ in Equation (10) gives the velocity distribution in the stripping section. For batch-type

operation, $\sigma_e = \sigma_s = A = 0$, and the velocity distribution for both enriching and stripping sections reduces to

$$v_z = \frac{\bar{\beta}_T \omega^2 (\Delta T) g \cos \phi}{12 \mu} (\eta - \eta^3) \quad . \tag{8'}$$

In this case, the right hand side of Equation (9) is equal to zero.

Some velocity profiles calculated from these equations are shown in Figure 3.

Concentration Distribution

The horizontal mass flux rate of component 1 of a binary mixture is related to the velocity by the differential mass balance equation

$$\frac{\partial J_x}{\partial x} + \bar{\rho} \, v_z \frac{\partial c}{\partial z} = 0 \quad ,$$

or

$$\frac{\partial J_x}{\partial \eta} + \bar{\rho} \, \omega \, v_z \frac{\partial c}{\partial z} = 0 \quad . \tag{11}$$

In writing this equation, the assumptions are made that diffusion in the z-direction is negligible, that bulk flow in the x-direction is negligible, and that the concentration at a point is independent of time.

The net flow due to thermal diffusion and ordinary diffusion in the x-direction must be zero at both walls. Therefore, a solution to Equation (11) must be found subject to the boundary conditions

$$\text{at } \eta = \pm 1, \quad J_x = 0 \quad . \tag{12}$$

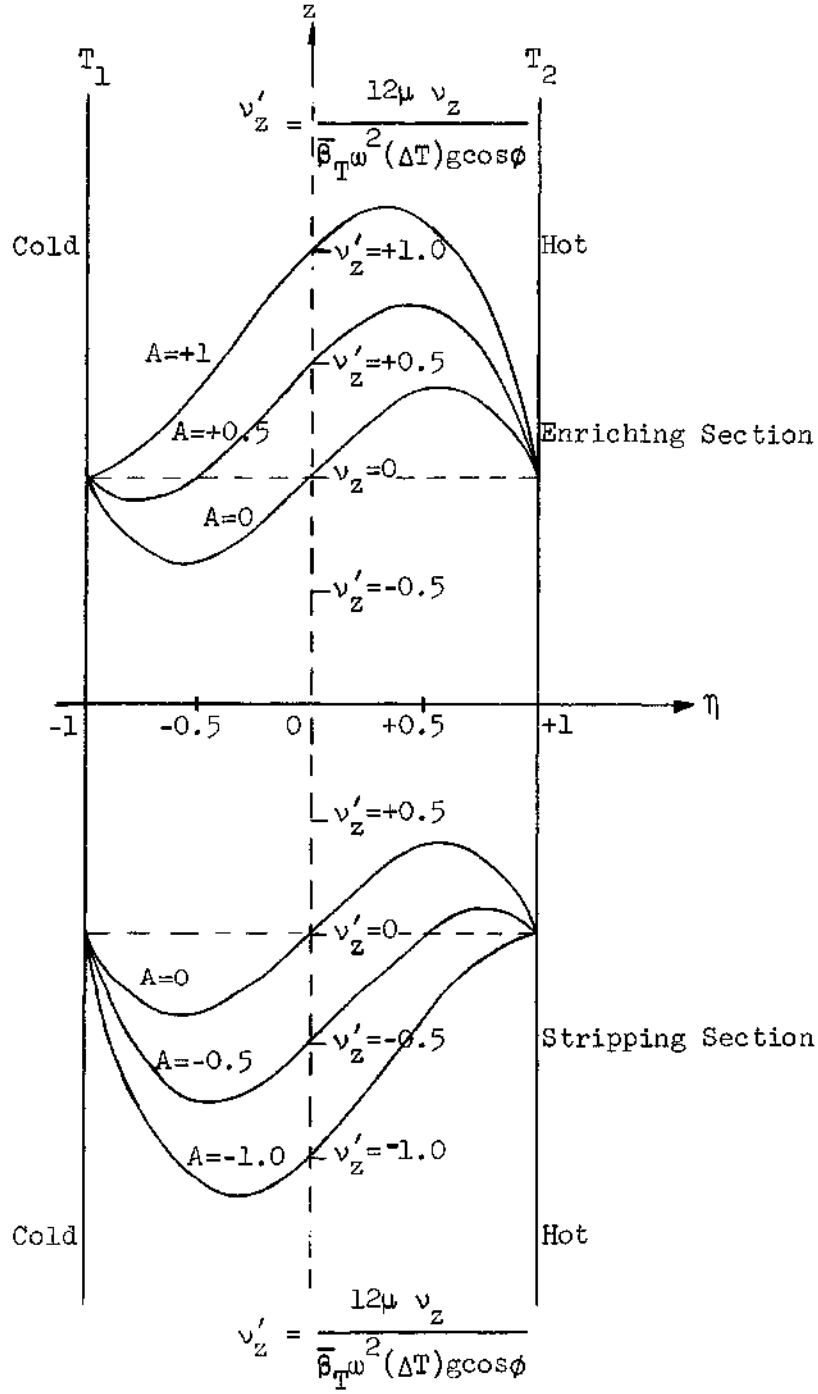

Figure 3. Velocity Distributions of Fluid Flowing Between the Hot and Cold Walls of a Wired Concentric Tube Thermal Diffusion Column with Flow Rate as Parameter

In obtaining a solution to these equations for batch operation ($\sigma_e = \sigma_s = 0$) in a parallel plate thermal diffusion column, Furry, Jones, and Onsager[9,10] assumed $\frac{\partial c}{\partial z}$ in Equation (11) to be independent of x. However, this assumption is incompatible with the boundary conditions, Equation (12), in the case of a continuous flow column.

It is assumed in the course of this work that $\frac{\partial c}{\partial z}$ is not independent of x but varies linearly with x, according to

$$\frac{\partial c}{\partial z} = (1+\gamma\eta)\ \Psi(z) \quad , \tag{13}$$

in which γ is a constant to be determined. This assumption makes it possible to satisfy the boundary conditions imposed by Equation (12). Completing the integration of Equation (11) yields the net mass flux in the horizontal direction in the enriching section, as follows:

$$J_x = \frac{\overline{\rho}\ \overline{\beta}_T\ \omega^3(\Delta T)g\cos\phi}{12\ \mu}\ \Psi(z)\left[(1-5A^2)\left(\frac{\eta^2}{2} - \frac{\eta^4}{4} - \frac{1}{4}\right) + A(\eta - 2\eta^3 + \eta^5)\right] \tag{14}$$

and Equation (13) becomes

$$\frac{\partial c}{\partial z} = (1-5A\ \eta)\ \Psi(z) \quad . \tag{13'}$$

In addition, the expression for J_x in terms of the two contributions, ordinary and thermal diffusion, is

$$J_x = D\ \overline{\rho}\left(-\frac{\partial c}{\partial x} + \frac{\alpha c\overline{c}}{T}\frac{dT}{dx}\right) \quad ,$$

or

$$J_x = \frac{D\,\bar{\rho}}{\omega}\left(- \frac{\partial c}{\partial \eta} + \frac{\alpha c \bar{c}}{T}\frac{dT}{d\eta} \right) \quad , \tag{15}$$

from which the concentration profile may be calculated by equating Equations (14) and (15) and integrating with the following boundary conditions:

$$\text{at } \eta = \eta \quad , \qquad c = c(\eta, z) \tag{16}$$

$$\text{at } \eta = 0 \quad , \qquad c = c_o(0, z) \quad . \tag{17}$$

The solution is

$$c = c_o + \frac{\alpha c \bar{c}(\Delta T)}{2\,\bar{T}}\,\eta - \frac{\bar{\beta}_T\,\omega^4(\Delta T)\,g\cos\phi}{12\,D\mu}\,\Psi(z)\left[(1-5A^2)\left(\frac{\eta^3}{6} - \frac{\eta^5}{20} - \frac{\eta}{4} \right) + A\left(\frac{\eta^2}{2} - \frac{\eta^4}{2} + \frac{\eta^6}{6} \right) \right] \quad . \tag{18}$$

In obtaining the above solution, it was assumed that the quantity $\frac{\alpha c \bar{c}}{T}$ appearing in the thermal diffusion term was independent of x, and $\frac{dT}{d\eta}$ was obtained from Equation (6).

Equations (18) and (10) represent the steady-state concentration distribution of a binary solution in the enriching section of a wired concentric tube thermal diffusion column under continuous operation, while, replacing σ_e with $-\sigma_s$ gives the steady-state concentration distribution in the stripping section. For batch-type operation, $\sigma_e = \sigma_s = A = 0$, and the concentration distribution for both enriching and stripping sections reduces to

$$c = c_o + \frac{\alpha c \bar{c} (\Delta T)}{2 \bar{T}} \eta - \frac{\bar{\beta}_T \omega^4 (\Delta T) g \cos \phi}{12 D \mu} \Psi(z) \left[\frac{\eta^3}{6} - \frac{\eta^5}{20} - \frac{\eta}{4} \right] \quad . \qquad (19)$$

Transport Equation

The rate of mass transport of component 1 in the z-direction is given by

$$\tau_1 = \int_{-\omega}^{+\omega} \bar{\rho} \, c \, v_z \, B \, dx - \int_{-\omega}^{+\omega} \bar{\rho} \, D \, \frac{\partial c}{\partial z} \, B \, dx \quad ,$$

or

$$\tau_1 = \bar{\rho} \, B \, \omega \int_{-1}^{+1} c \, v_z \, d\eta - \bar{\rho} \, D \, B \, \omega \, \Psi(z) \int_{-1}^{+1} (1 - 5A \, \eta) \, d\eta \qquad (20)$$

Combining Equations (8), (18), and (20), and integrating, one obtains, by replacing $\Psi(z)$ with $\frac{dc_o}{dz}$ and making use of Equation (9)

$$\tau_1 = c_o \, \sigma_e + H c \bar{c} - K_e \frac{dc_o}{dz} \quad , \qquad (21)$$

where

$$H = \frac{\alpha \, \bar{\beta}_T \, \bar{\rho} \, g \cos \phi (2\omega)^3 \, B \, (\Delta T)^2}{6! \, \mu \, \bar{T}} \qquad (22)$$

$$K_e = K_{ce} + K_d \qquad (23)$$

$$K_{ce} = \frac{\bar{\beta}_T^2 \, \bar{\rho} \, g^2 \cos^2 \phi \, (2\omega)^7 \, B \, (\Delta T)^2}{9! \, D \mu^2} \left[1 + \frac{41}{24} A - 5A^2 \right] \qquad (24)$$

$$K_d = 2\omega\ D\ B\ \bar{\rho} \quad . \tag{25}$$

In Equation (21), τ_1 is the transport of component 1 in the positive z-direction in the enriching section under steady, continuous operation. The transport coefficients H and K_e are constants which, shown in Equations (22), (23), (24), and (25), depend on the nature of the gas or liquid, on the pressure in the case of a gas, on the dimensions and shape of the apparatus, on the temperature difference maintained in the column, and on the flow rate. They do not depend on τ_1, c_o, or z.

By making a similar analysis, the transport of component 1 in the negative z-direction in the stripping section under steady, continuous operation is obtained as

$$\tau_1 = - c_o \sigma_s + Hc\bar{c} - K_s \frac{dc_o}{dz} \quad , \tag{26}$$

in which

$$K_s = K_e \Big|_{\sigma_e \rightarrow -\sigma_s} \quad . \tag{27}$$

Equation of Separation

Usually the variation of c with x need not be considered in any of the applications of the transport equation. It is not that the small transverse variation of c is not important, but rather that its effect is taken into account by the coefficients H and K_e, or K_s, and need not be considered further. In other words, since $|\ c(-1,z) - c(+1,z)\ |$ is small, as compared with the concentration difference between

the top and bottom ends, we may make the approximation, $c_o(0,z) \approx c_b(z)$, in which $c_b(z)$ is defined by

$$c_b(z) = \frac{\bar{\rho}B}{\sigma_e} \int_{-\omega}^{+\omega} c\, v_z\, dx \tag{28}$$

in the enriching section, and

$$c_b(z) = \frac{\bar{\rho}B}{-\sigma_s} \int_{-\omega}^{+\omega} c\, v_z\, dx \tag{29}$$

in the stripping section. By making this approximation, Equations (21) and (26) can be rewritten, respectively, as

$$\tau_1 = \sigma_e\, c_b + Hc\bar{c} - K_e \frac{dc_b}{dz} \quad , \tag{30}$$

and

$$\tau_1 = -\sigma_s\, c_b + Hc\bar{c} - K_s \frac{dc_b}{dz} \quad . \tag{31}$$

The three terms in each of the transport equations, Equations (30) and (31), all have simple interpretations: the first two terms represent the mass transport contributed by bulk flow and thermal diffusion, respectively; the last term represents remixing due to the flow of fluid and ordinary diffusion along the transport direction.

Since at steady-state, τ_1, σ_e, and σ_s are constants, and $\frac{\tau_1}{\sigma_e} = c_{fe}$, and $\frac{\tau_1}{-\sigma_s} = c_{fs}$ everywhere in the enriching section and the stripping section, respectively, Equations (30) and (31) become, respectively:

$$H\left[c\bar{c} - \frac{\sigma_e}{H}(c_{fe}-c_b)\right] = K_e \frac{dc_b}{dz} \tag{32}$$

$$H\left[c\bar{c} + \frac{\sigma_s}{H}(c_{fs}-c_b)\right] = K_s \frac{dc_b}{dz} \quad . \tag{33}$$

The integration of Equation (32) with $c\bar{c}$ held constant which staisfies the boundary conditions

$$\text{at } z = 0, \qquad c_b = c_i \tag{34}$$

$$\text{at } z = z_{fe}, \quad c_b = c_{fe} \tag{35}$$

is

$$c_{fe} - c_i = c\bar{c}\left(1 - e^{-\frac{\sigma_e z_{fe}}{K_e}}\right) H/\sigma_e \quad . \tag{36}$$

Similarily, the integration of Equation (33) with $c\bar{c}$ held constant which satisfies the boundary conditions

$$\text{at } z = 0, \qquad c_b = c_i \tag{37}$$

$$\text{at } z = -z_{fs}, \quad c_b = c_{fs} \tag{38}$$

is

$$c_{fs} - c_i = -c\bar{c}\left(1 - e^{-\frac{\sigma_s z_{fs}}{K_s}}\right) H/\sigma_s \quad . \tag{39}$$

Combining Equation (36) with Equation (39) we obtain

$$\Delta = c_{fe} - c_{fs} = c\bar{c}\left[\left(1 - e^{-\frac{\sigma_e z_{fe}}{K_e}}\right) H/\sigma_e + \left(1 - e^{-\frac{\sigma_s z_{fs}}{K_s}}\right) H/\sigma_s\right] \tag{40}$$

For the important case in which c is everywhere within the range 0.3 to 0.7, and in which therefore $c\bar{c}$ is never far from $\frac{1}{4}$, Equation (40) becomes:

$$\Delta = \left(1 - e^{-\frac{\sigma_e z_{fe}}{K_e}}\right) H/4\sigma_e + \left(1 - e^{-\frac{\sigma_s z_{fs}}{K_s}}\right) H/4\sigma_s \quad . \tag{41}$$

Equation (41) is the equation of separation of a binary solution in a continuous wired concentric tube thermal diffusion column operating under steady-state conditions.

Equation of Separation in a Practical Wired Concentric Tube Column

Since operation at high flow rates in a continuous thermal diffusion column is very inefficient, moderate flow rates are usually used. Hence, neglecting the flow rate terms in the transport coefficients, K_e and K_s, should not lead to serious error. Furthermore, the term K_d, representing remixing due to ordinary diffusion in the transport direction, is generally negligible compared with the convection term K_c given in Equation (23). In this case,

$$K = K_e = K_s = \frac{\bar{\rho}\,\bar{\beta}_T^2\, g^2 \cos\phi\, (2\omega)^7\, B(\Delta T)^2}{9!\, D\mu^2} \quad . \tag{23'}$$

It will be shown later by the experimental results in Chapter V

that the above simplification is reasonable. If, in addition, the feed is introduced at the midpoint of the column, i.e., $z_{fe} = z_{fs} = \frac{1}{2} L$, and the flow rates both in the enriching section and the stripping section are kept the same, i.e., $\sigma = \sigma_e = \sigma_s$, then Equation (41) becomes

$$\Delta = \frac{H}{2\sigma}\left[1 - \exp\left(-\frac{\sigma L}{2K}\right)\right] \quad . \tag{42}$$

Note that Equation (42) reduces to that obtained in a vertical parallel plate column by Jones, Furry, and Onsager[9,10], if we set $\phi = 0$. The column length L of a parallel plate thermal diffusion column obtained from a concentric tube column with a wire spiral inserted as a spacer in the annulus, is equal to the column height of the concentric tube thermal diffusion column times sec ϕ, or $L = h \sec \phi$. As mentioned earlier in this chapter, because of the diminutive size of the annular spacing, the wire diameter is very small as compared with the wire spacing except when the angle of inclination ϕ of the wire spiral approaches 90°. However, the separation is something like that in the static system when ϕ approaches 90°. In this case, the degree of separation is generally so slight that it is of no practical interest. Therefore, we neglect the space occupied by the wire spiral inserted in the annulus and set $BL = 2\pi R_1 h$, or $B = 2\pi R_1 \cos \phi$. By modifying Equation (42) with these relations and replacing (2ω) with $(R_2 - R_1)$, we obtain the separation equation of a binary solution in a practical continuous wired concentric tube thermal diffusion column operating under steady-state conditions, as:

$$\Delta = \frac{H_o \cos^2 \phi}{2\sigma} \left[1 - \exp\left(- \frac{\sigma h}{2K_o \cos^4 \phi} \right) \right] \tag{43}$$

where

$$H_o = \frac{\alpha \bar{\rho} \bar{\beta}_T g(R_2-R_1)^3(2\pi R_1)(\Delta T)^2}{6! \mu \bar{T}} \tag{44}$$

$$K_o = \frac{\bar{\rho} \bar{\beta}_T^2 g^2(R_2-R_1)^7(2\pi R_1)(\Delta T)^2}{9! D\mu^2} \quad . \tag{45}$$

Setting $\phi = 0$ in Equation (43) gives

$$\Delta_o = \frac{H_o}{2\sigma} \left[1 - \exp\left(- \frac{\sigma h}{2K_o} \right) \right] \quad , \tag{46}$$

which is the separation equation for an open column.

The Optimum Wire Angle for Maximum Separation

The optimum angle of inclination of a spiral wire for maximum separation in a practical wired concentric tube column, is obtained by partially differentiating Equation (43) with respect to ϕ and setting $\frac{\partial \Delta}{\partial \phi} = 0$. After simplification, this gives

$$e^X = 2X + 1 \quad , \tag{47}$$

where

$$X = \frac{\sigma h}{2K_o \cos^4 \phi_{opt}} \quad . \tag{48}$$

Solving for X, gives X = 1.26,0. The root, X = 0 has no physical meaning and is therefore discarded.

The optimum angle of inclination of a spiral wire can be obtained by substituting X = 1.26 into Equation (48):

$$\phi_{opt} = \cos^{-1}\left(\frac{\sigma h}{2.52\ K_o}\right)^{\frac{1}{4}} \quad . \tag{49}$$

If Equation (49) is substituted into Equation (43), the maximum separation obtainable is given by the following expression

$$\Delta_{max} = 0.226\left(\frac{H_o^2 h}{K_o \sigma}\right)^{\frac{1}{2}} \quad . \tag{50}$$

There is an important restriction on the existence of the best wire angle of inclination for maximum separation. Since $0 < \phi < \frac{\pi}{2}$, it follows that $\cos \phi < 1$, and from Equation (49) one obtains the inequality, $\sigma < 2.52\ \frac{K_o}{h}$. Thus, if $\sigma > 2.52\ \frac{K_o}{h}$, Equation (49) has no real solution, and in that event there is no best wire angle of inclination which will give maximum separation. Also, from the assumptions used to obtain Equation (43), $\Delta < 0.4$, and by Equation (50), $\sigma > \frac{0.319\ H_o^2 h}{K_o}$. If σ is smaller than this value, Equation (50) is inapplicable. Thus, Equations (49) and (50) are applicable in the range of

$$\frac{0.319\ H_o^2 h}{K_o} < \sigma < \frac{2.52\ K_o}{h} \quad . \tag{51}$$

Graphical Representation

The equation of separation and the solution of the conditions

for the best performance can be most conveniently represented graphically in terms of dimensionless variables. We define the dimensionless flow rate σ' and reduced separation Δ' by

$$\sigma' = \frac{\sigma h}{K_o} \tag{52}$$

$$\Delta' = \frac{\Delta\sigma}{H_o} \quad . \tag{53}$$

Equations (43), (49), and (50) can then be written as

$$\Delta' = \frac{\cos^2 \phi}{2}\left(1 - e^{-\frac{\sigma'}{2\cos^4 \phi}} \right) \tag{54}$$

$$\phi_{opt} = \cos^{-1}\left(\frac{\sigma'}{2.52} \right)^{\frac{1}{4}} \tag{55}$$

and

$$\Delta'_{max} = 0.226(\sigma')^{\frac{1}{2}} \quad . \tag{56}$$

By eliminating σ' in Equations (55) and (56), the result is

$$\Delta'_{max} = 0.358 \cos^2(\phi_{opt}) \quad . \tag{57}$$

Figure 4 is the graphical representation of Equation (54) and Figure 5 is the graphical representation of Equations (55) and (56). Equation (57) is also plotted in Figure 4 as a dotted line.

It should be noted that for $\sigma' > 2.52$, no optimum wire angle exists

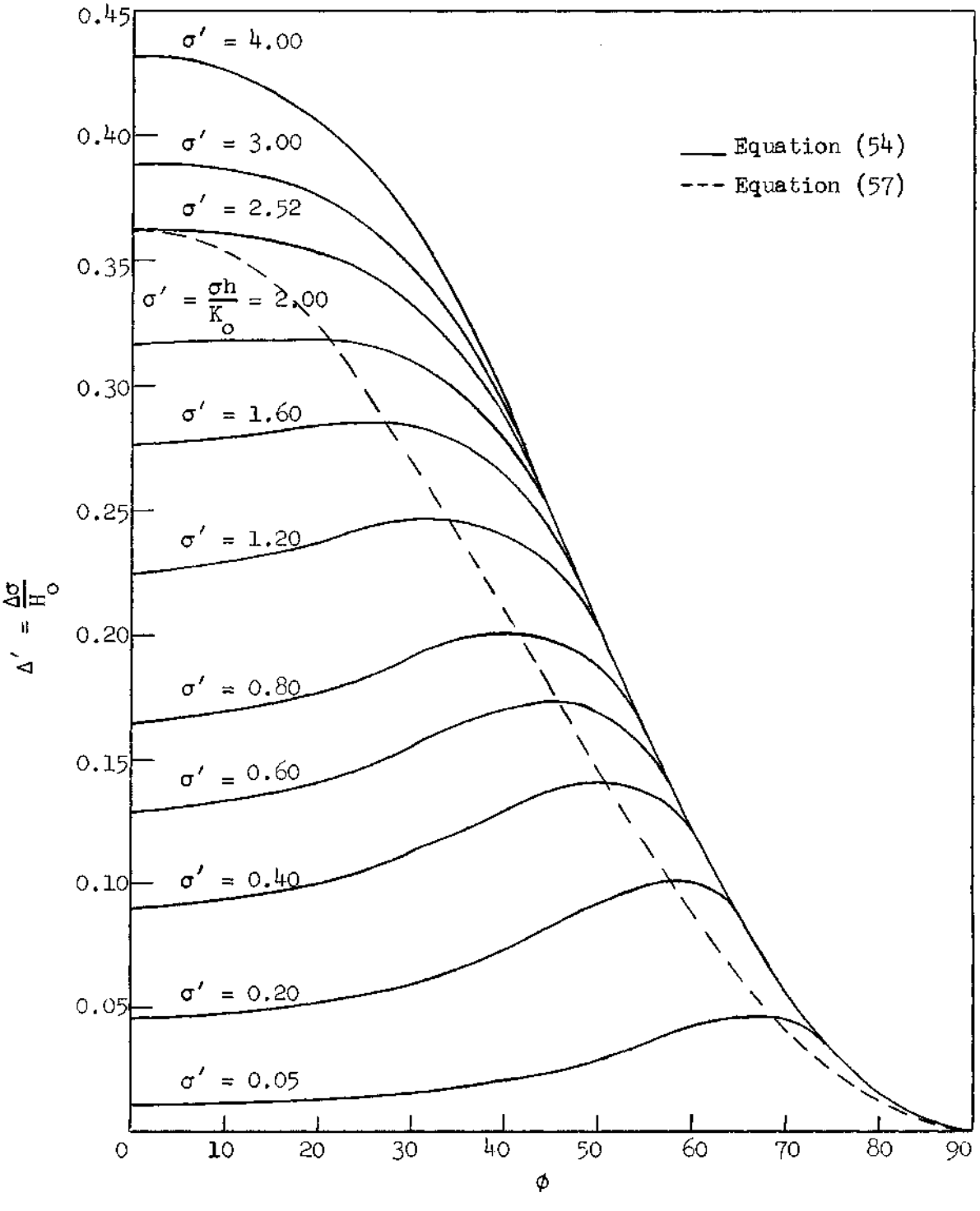

Figure 4. Effect of Wire Angle of Inclination on the Separation at Constant Flow Rate

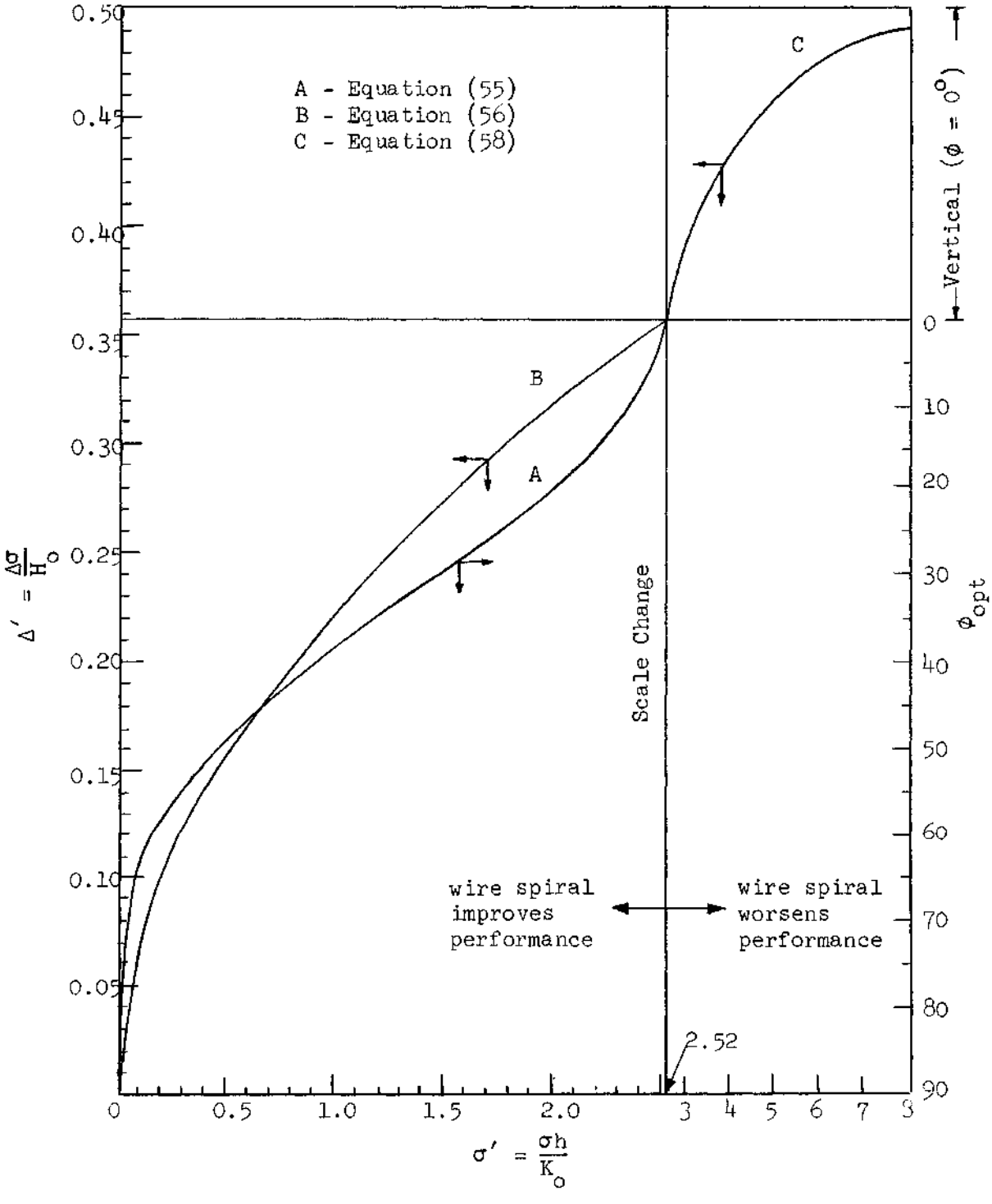

Figure 5. Wire Angle of Inclination for Best Performance Versus Reduced Flow Rate and Reduced Separation

and the best separation is obtained when there is no wire spiral inserted in the annulus of the concentric tube column ($\phi = 0$). Under such conditions, Equation (54) reduces to

$$\Delta' = \frac{1}{2}\left(1 - e^{-\frac{\sigma'}{2}}\right) . \tag{58}$$

This is also plotted in the upper right corner of Figure 5.

Evaluation of Constants H_o and K_o

For a given system, H_o and K_o are constants which may be found from Equations (44) and (45). Unfortunately, some of the physical constants required for the evaluation of H_o and K_o are not readily available. These two transport coefficients can be most easily evaluated from two experimental runs at the same wire angle of inclination.

If Equation (43) is applied to two sets of data with the same wire angle of inclination, with the condition that $\sigma_B = 2\,\sigma_A$, then

$$\Delta_A = \frac{H_o \cos^2 \phi}{2\,\sigma_A}\left[1 - \exp\left(-\frac{\sigma_A h}{2\,K_o \cos^4 \phi}\right)\right] \tag{59}$$

$$\Delta_B = \frac{H_o \cos^2 \phi}{2\,\sigma_B}\left[1 - \exp\left(-\frac{\sigma_B h}{2\,K_o \cos^4 \phi}\right)\right] . \tag{60}$$

Solving Equations (59) and (60) for H_o and K_o with the condition that $\sigma_B = 2\,\sigma_A$, gives

$$H_o = \frac{\sigma_A\,\Delta_A^2}{\left(\Delta_A - \Delta_B\right)\cos^2 \phi} \tag{61}$$

$$K_o = \frac{\sigma_A h}{2 \cos^4 \phi \ln\left(\frac{\Delta_A}{2\Delta_B - \Delta_A}\right)} \tag{62}$$

If the two sets of experimental data are obtained from a column without a wire spiral, then Equations (61) and (62) reduce to

$$H_o = \frac{\sigma_A \Delta_A^2}{\Delta_A - \Delta_B} \tag{63}$$

$$K_o = \frac{\sigma_A h}{2 \ln\left(\frac{\Delta_A}{2\Delta_B - \Delta_A}\right)} \quad . \tag{64}$$

CHAPTER III

EXPERIMENTAL EQUIPMENT AND INSTRUMENTATION

A concentric tube thermal diffusion column was constructed as shown in Figures 6 and 7. The main body of this column, made of two stainless steel tubes, had a fractionating section of 22 inches and an annular space of 0.0325 inch. The outside diameter of the inner tube was 1.315 inches, while the inside diameter of the outer tube was 1.380 inches. The system to be separated flowed through the annular region. A tight fitting wire spiral, having a diameter equal to the annular spacing was wrapped on the entire inner tube. The wires employed were stainless steel. To apply the wire, the inner tube was removed from the column and placed in a horizontal position. After the desired spacing was marked, the wire was wrapped in a spiral manner on the entire inner tube and finally fastened to the tube by small amounts of epoxy glue. After the glue dried, the inner tube was inserted carefully into the outer tube. A small amount of the test mixture was used as a lubricant during insertion of the wire-wrapped inner tube. It should be emphasized that the wire spiral was not used as an electric heater, but rather as a guide and spacer within the annulus.

Two 5-inch OD flanges were welded on the outside surface at each end of the outer tube and a $6\frac{1}{2}$" OD flange was welded on the outside surface at the bottom end of the inner tube. A $2\frac{1}{2}$" OD cap and a $1\frac{1}{2}$" OD cap were screwed into the top and bottom of the inner tube, respectively,

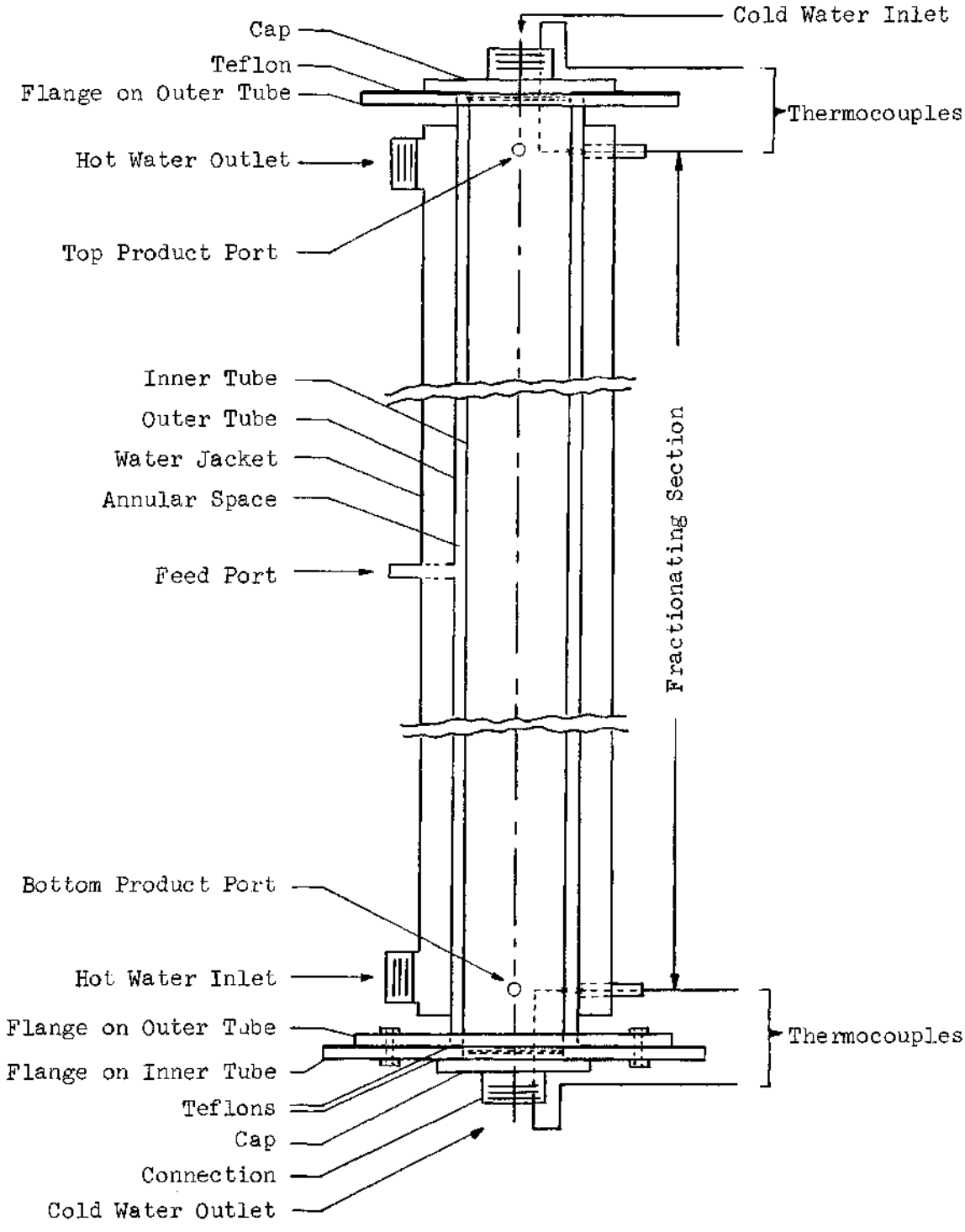

Figure 6. The Concentric Tube Thermal Diffusion Column

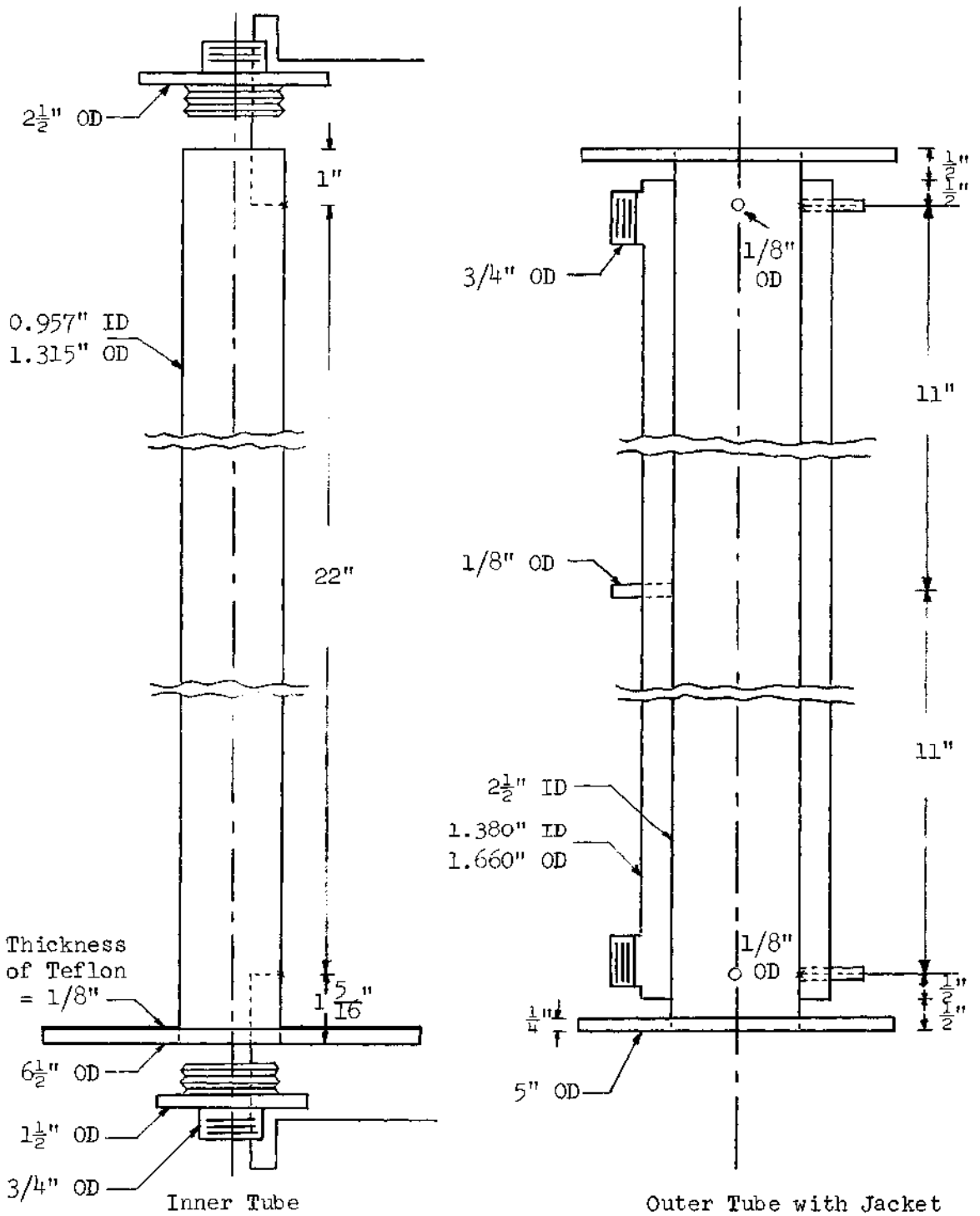

Figure 7. Dimensions of Concentric Tube Thermal Diffusion Column

using 1/8" thick teflon sheets as packing material between the flanges and caps. An additional teflon sheet was inserted between the flanges at the bottom of the column to seal the bottom of the annular space. Connections for 3/4" ID hose were provided in the top and bottom caps.

A 2½" ID jacket with 3/4" OD connections at the top and bottom was placed around the outer tube. This jacket was insulated with a 2" layer of asbestos insulation.

One-eighth inch OD holes were drilled at the midpoint and at the top and bottom of the column to serve as feed and product ports, respectively. Through each of these holes was passed 1/8" OD tubing which occupied a position connecting the particular point on the outer tube with the corresponding one on the jacket.

The outer and inner tubes were heated by hot and cold water, respectively. A system consisting of a 12-gallon tank, in which five 300-watt heaters were mounted, and a small centrifugal pump was provided for heating and circulating hot water through the jacket. One of these heaters was connected with a transformer to control the water temperature in the heating tank. Tap water was used for the cold water system.

Two copper constantan thermocouples were located on the surface of each tube at the inlet and outlet, respectively, to measure the surface temperatures of the tubes. The thermocouples located on the inside surface of the outer tube were attached with soft solder and passed through the jacket in which each thermocouple was protected by a small tube. The other two thermocouples, located on the outside surface of the inner tube, were also attached with soft solder and drawn through the inner tube, and came out at the position where the inner tube was

connected with the hoses.

Two Brooks-Mite rotameters with flow rate ranges of 0 ~ 16 cc/min of water were installed in the two product stream lines to control and measure the flow rates. A Baush and Lomb Abbe refractometer with temperature control was used to determine composition. This instrument can measure refractive indices with a precision of ± 0.0001.

CHAPTER IV

EXPERIMENTAL PROCEDURE

After the inner tube had been wrapped with wire at the desired angle of inclination and inserted into the outer tube, the column was connected, as shown in Figure 8. At the beginning of a run, hot and cold water streams were circulated through the jacket and inner tube, respectively to keep these surfaces at the desired temperatures. At the same time, the feed and product streams were turned on and set at the desired flow rates. The feed flowed steadily from a constant-head tank by gravity into the midpoint of the column. The flow rates of the two product streams were controlled by adjusting the needle valves on the rotameters and withdrawn continuously at constant and equal rates. The product streams passed through cooling coils and then through rotameters to product accumulators.

Samples of both streams were analyzed at 20-minute intervals until steady-state was reached as indicated by no change in the refractive index reading over a period of 1 hour. The flow rate was changed after each run. After the desired range of flow rates was covered, the wire angle of inclination was changed and new runs were carried out in the same manner.

Two test mixtures were employed in the experimental work. First, optical grade benzene and n-heptane were used. The choice of this particular system was based on their widely different refractive indices

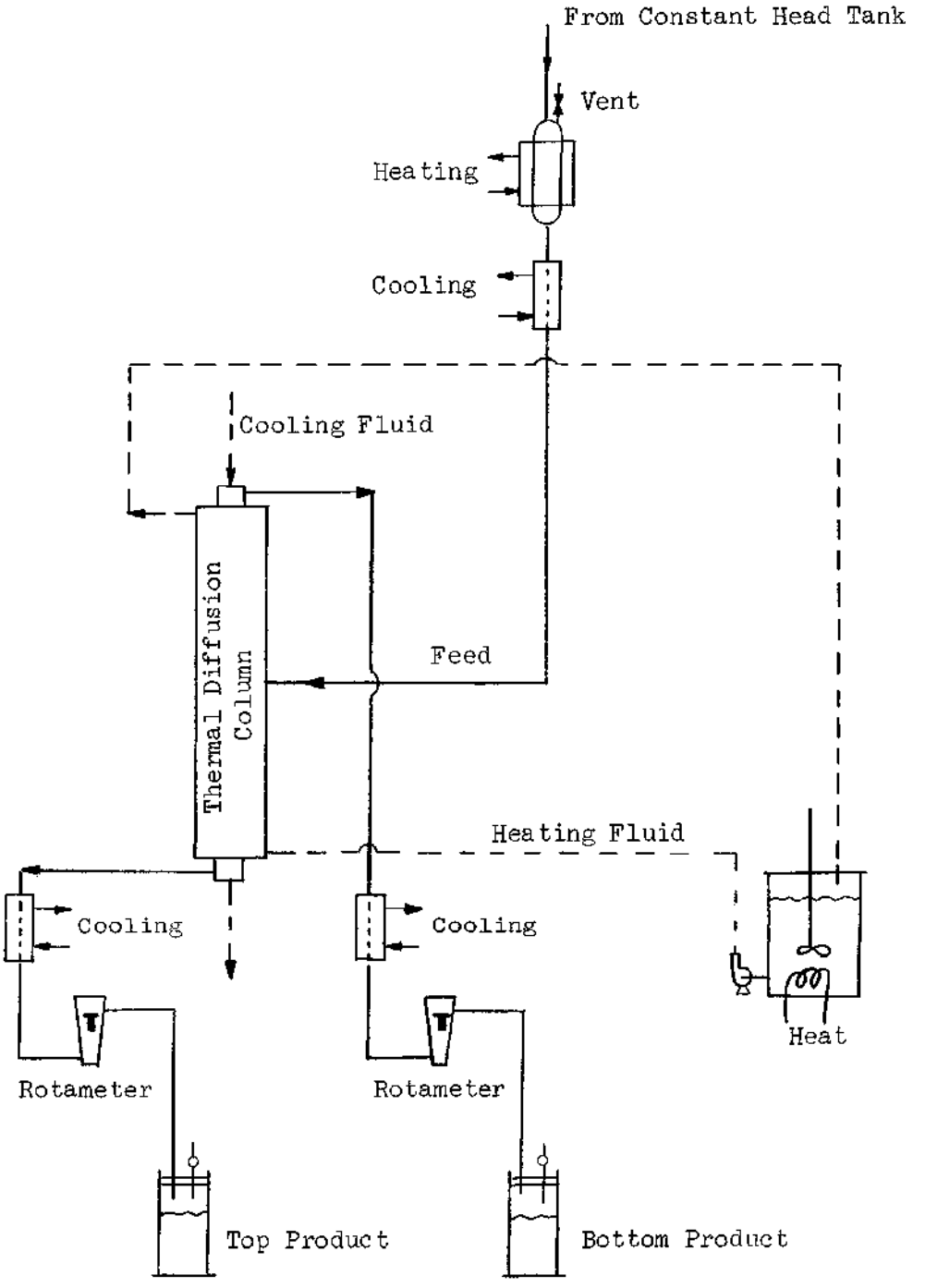

Figure 8. Flow Diagram of Wired Concentric Tube Thermal Diffusion Column

which made the analysis of composition by a refractometer possible and accurate. The feed consisting of 50 weight percent benzene and n-heptane was fed into the column. In the second experiment, optical grade toluene and isobutyl alcohol were used. In addition to their widely different refractive indices, this system has an azeotrope. The feed of this mixture was fed into the column at the azeotropic composition.

Two calibration curves of composition versus refractive index for each mixture were made using mixtures of known compositions. These two curves are shown in Appendix B. The Baush and Lomb Abbe refractometer used in this study can measure the composition with a precision of ± 0.1 percent for both test mixtures, based on the calibration curves.

CHAPTER V

EXPERIMENTAL RESULTS AND DISCUSSION

The experimental data obtained are tabulated in Tables 3 and 4 in Appendix A, and plotted in Figures 9 through 22.

For benzene-n-heptane mixtures, two data points near the low flow rate region in the run with $\phi = 45.5^{\circ}$ and a flow rate ratio of 2 were used to evaluate the system constants H_o and K_o. The experimental quantities are

$\sigma_A = 0.5$ g/min, $\Delta_A = 0.0820$ wt. fraction of n-heptane

$\sigma_B = 1.0$ g/min, $\Delta_B = 0.0545$ wt. fraction of n-heptane

h = 22 in., $\phi = 45.5$ deg, $\Delta T = 75^{\circ}$ F.

Substitution of these values into Equations (61) and (62) gives

$$H_o = 0.25 \text{ g/min} \tag{65}$$

$$K_o = 20.3 \text{ g in./min} \quad . \tag{66}$$

Substitution of these values into Equation (43) results in

$$\Delta = \frac{0.125 \cos^2 \phi}{\sigma} \left[1 - e^{-\frac{0.542\ \sigma}{\cos^4 \phi}} \right]. \tag{67}$$

Equation (67) is then the separation equation for benzene-n-heptane mixtures for all wire angles of inclination and all flow rates for

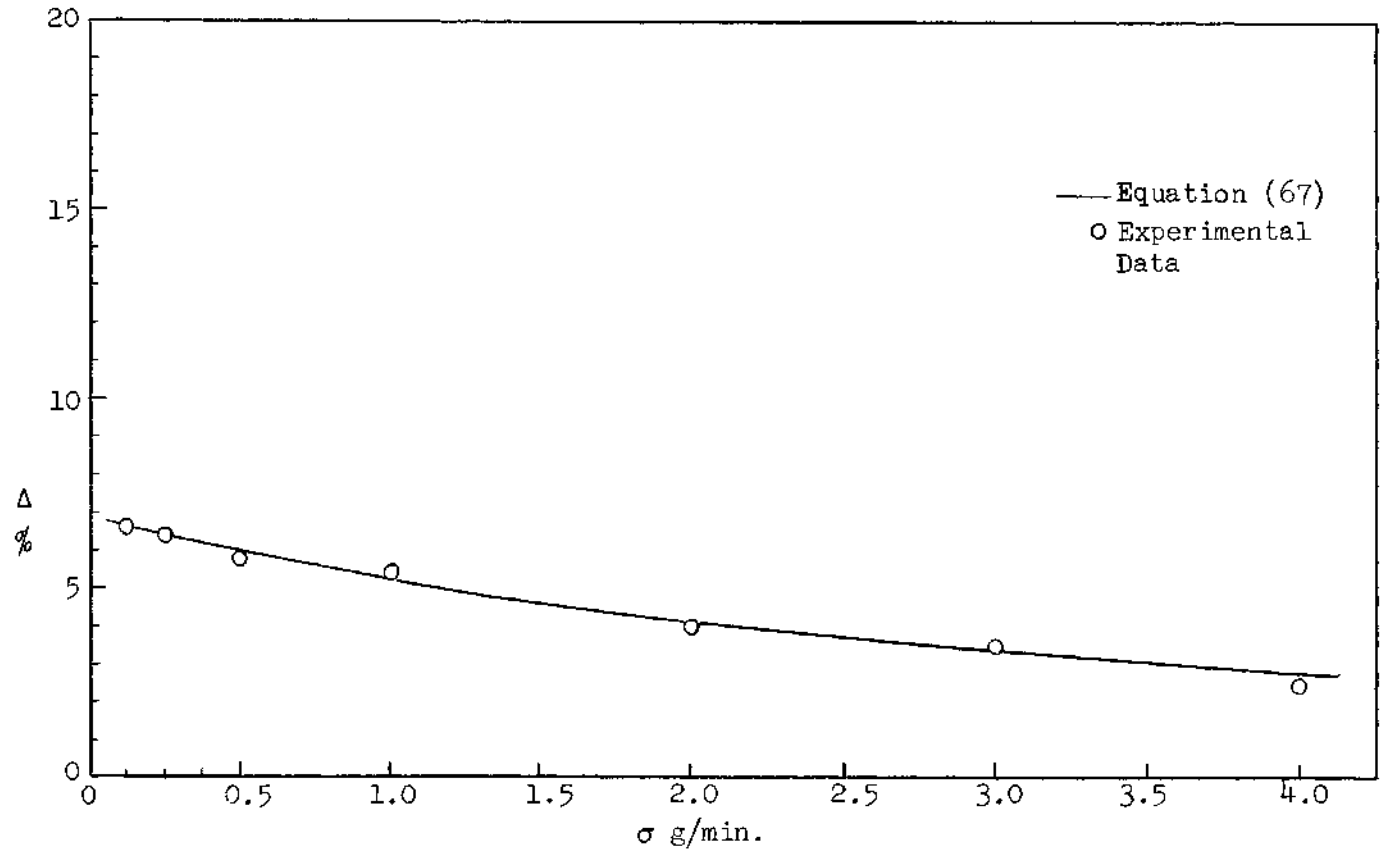

Figure 9. Degree of Separation of Equal Weight Fraction of Benzene-n-Heptane Mixture Versus Flow Rate at $\phi = 0^{o}$

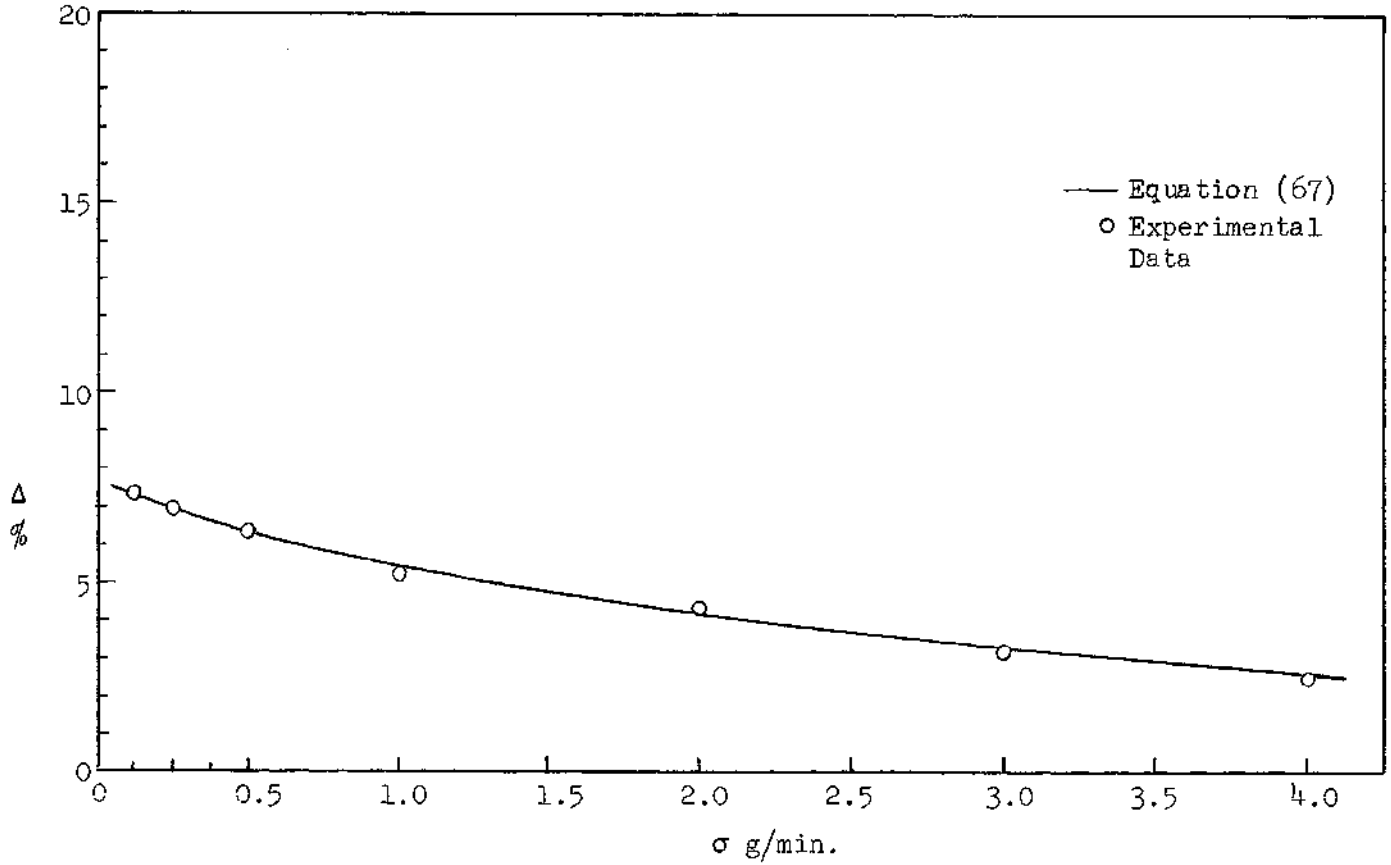

Figure 10. Degree of Separation of Equal Weight Fraction of Benzene-n-Heptane Mixture Versus Flow Rate at $\phi = 17.5^{\circ}$

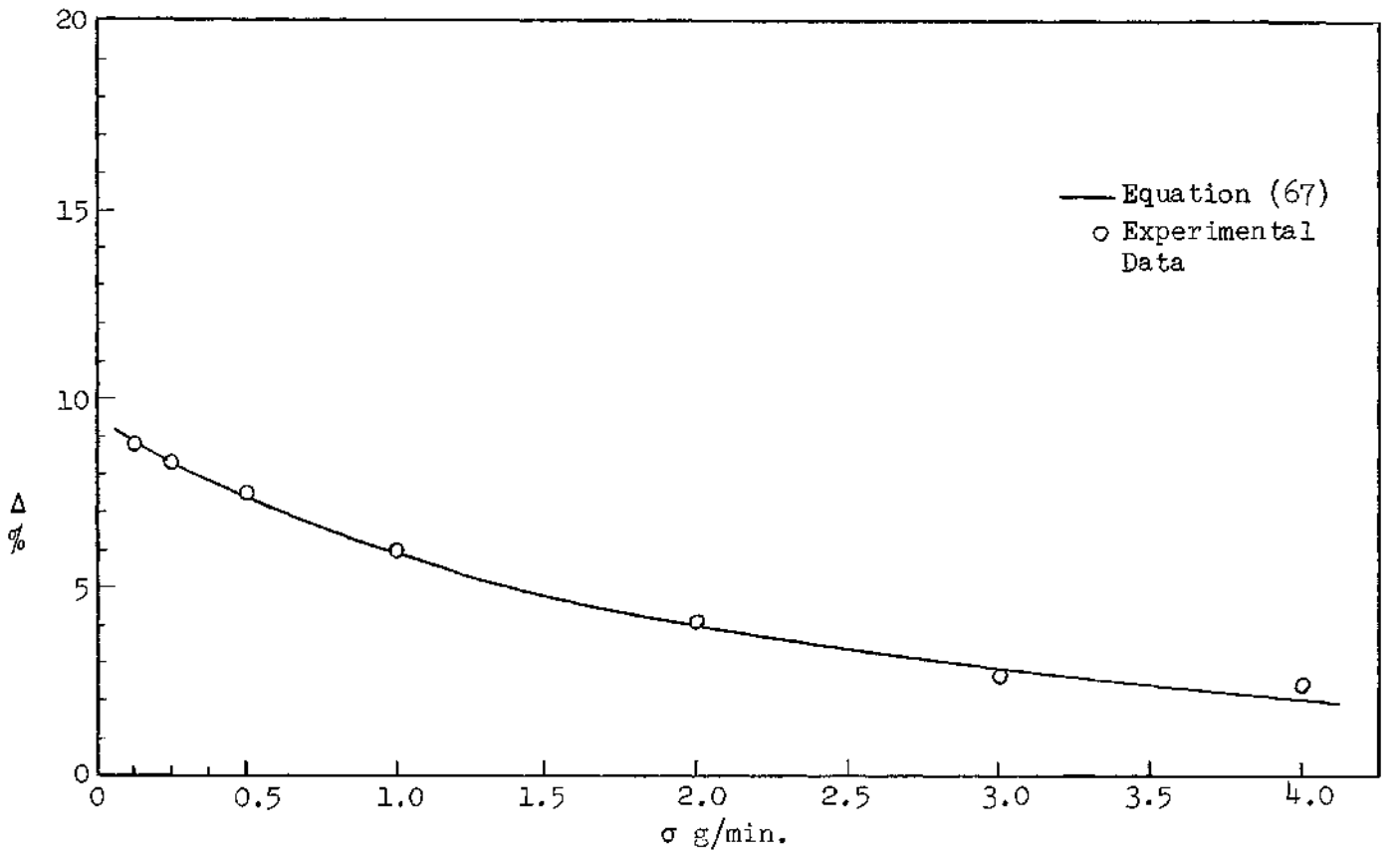

Figure 11. Degree of Separation of Equal Weight Fraction of Benzene-n-Heptane Mixture Versus Flow Rate at $\phi = 32^{\circ}$

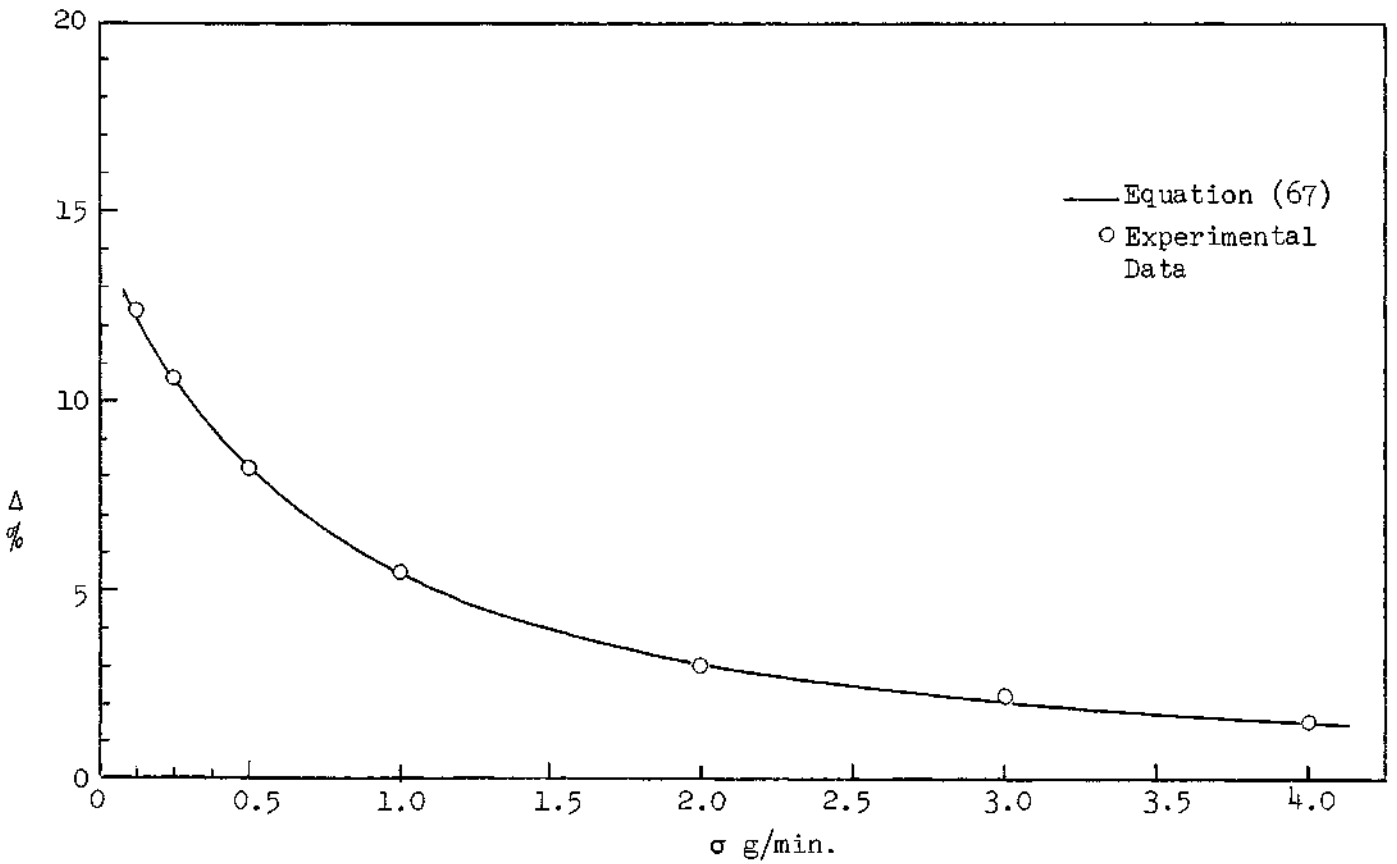

Figure 12. Degree of Separation of Equal Weight Fraction of Benzene-n-Heptane Mixture Versus Flow Rate at $\phi = 45.5^{\circ}$

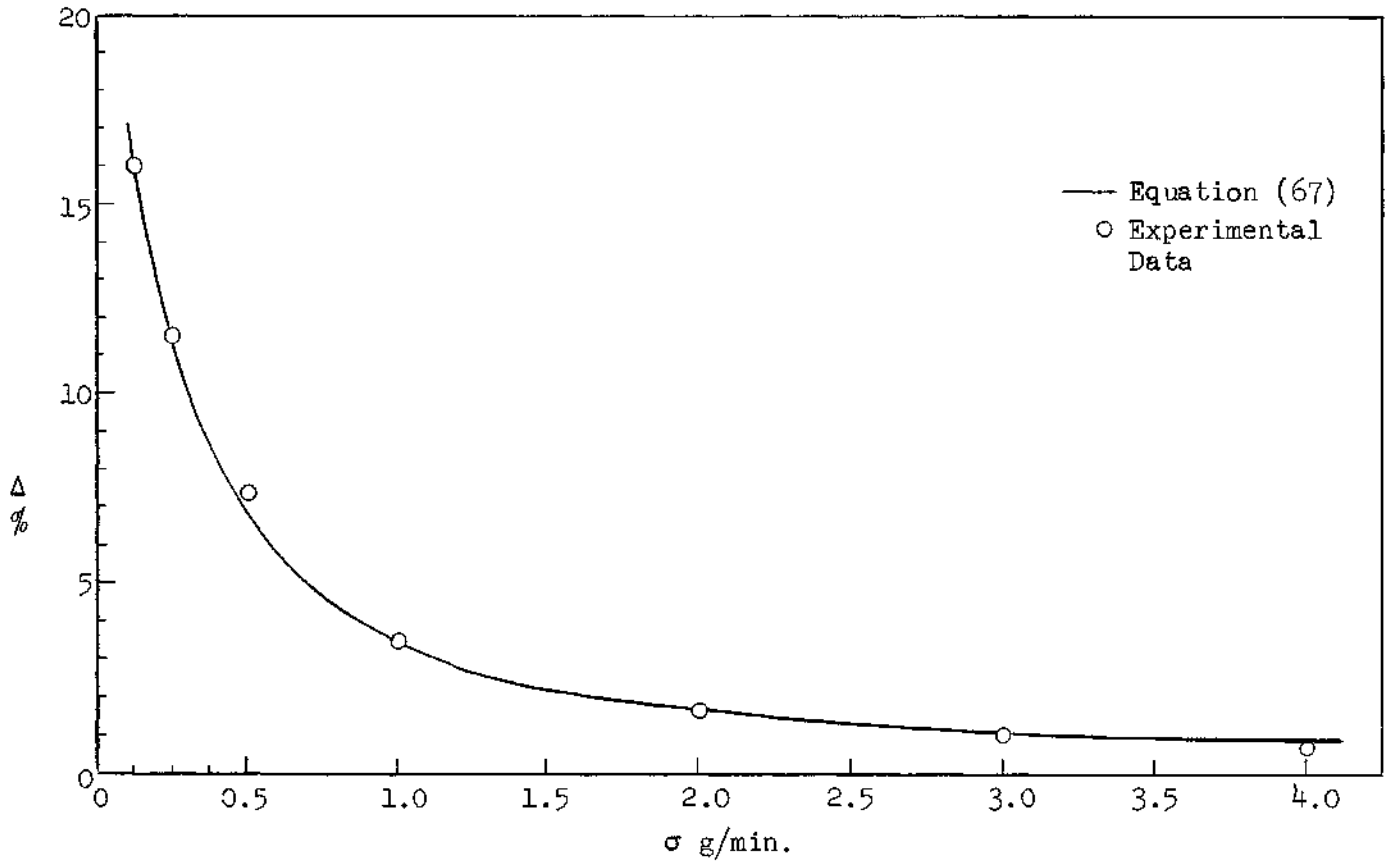

Figure 13. Degree of Separation of Equal Weight Fraction of Benzene-n-Heptane Mixture Versus Flow Rate at $\phi = 58^{\circ}$

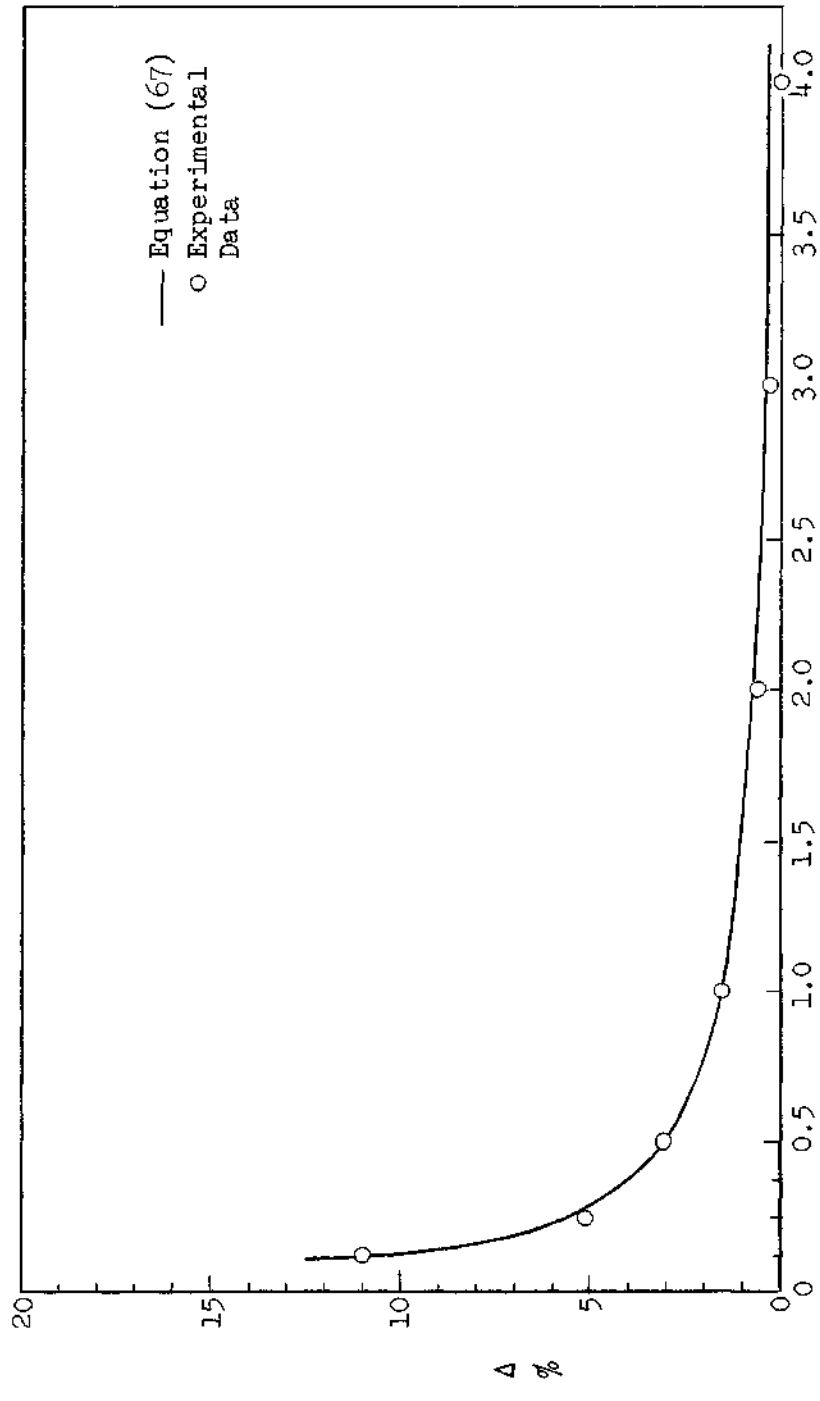

Figure 14. Degree of Separation of Equal Weight Fraction of Benzene-n-Heptane Mixture Versus Flow Rate at $\phi = 70^{\circ}$

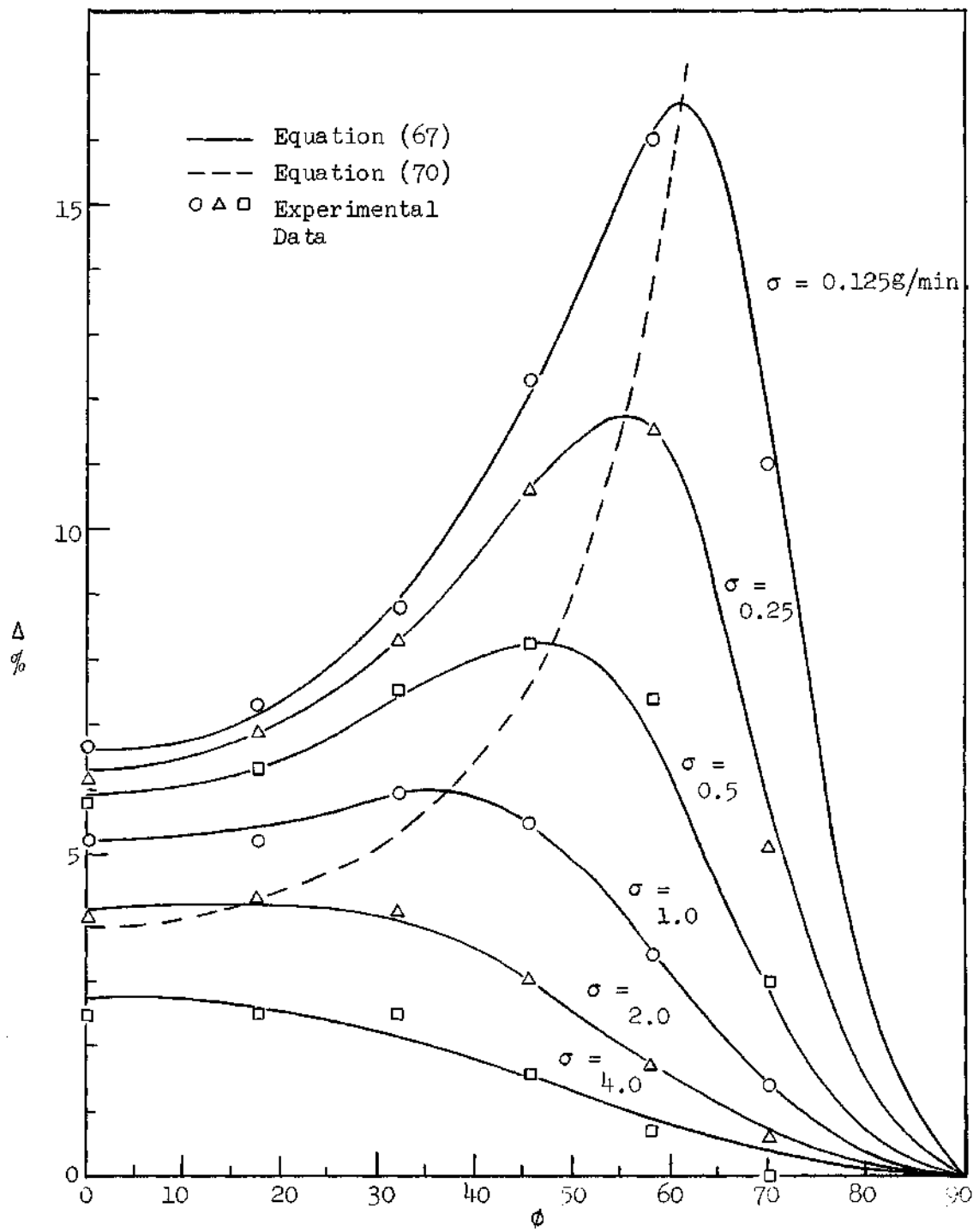

Figure 15. Effect of Wire Angle of Inclination on Degree of Separation for Equal Weight Fraction of Benzene-n-Heptane Mixture Obtained at Various Flow Rates

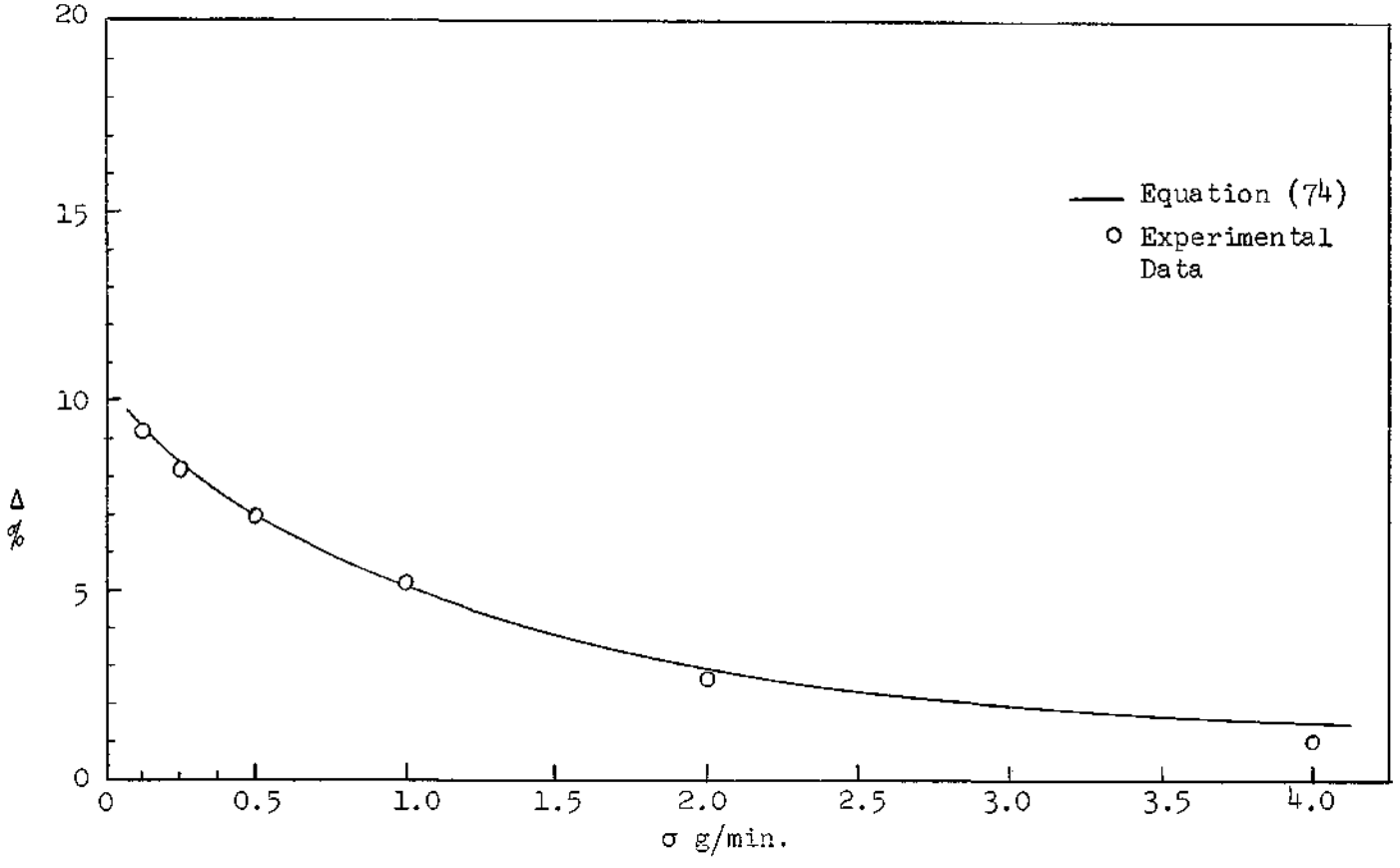

Figure 16. Degree of Separation of Toluene-Isobutyl Alcohol Azeotropic Mixture Versus Flow Rate at $\phi = 0^{o}$

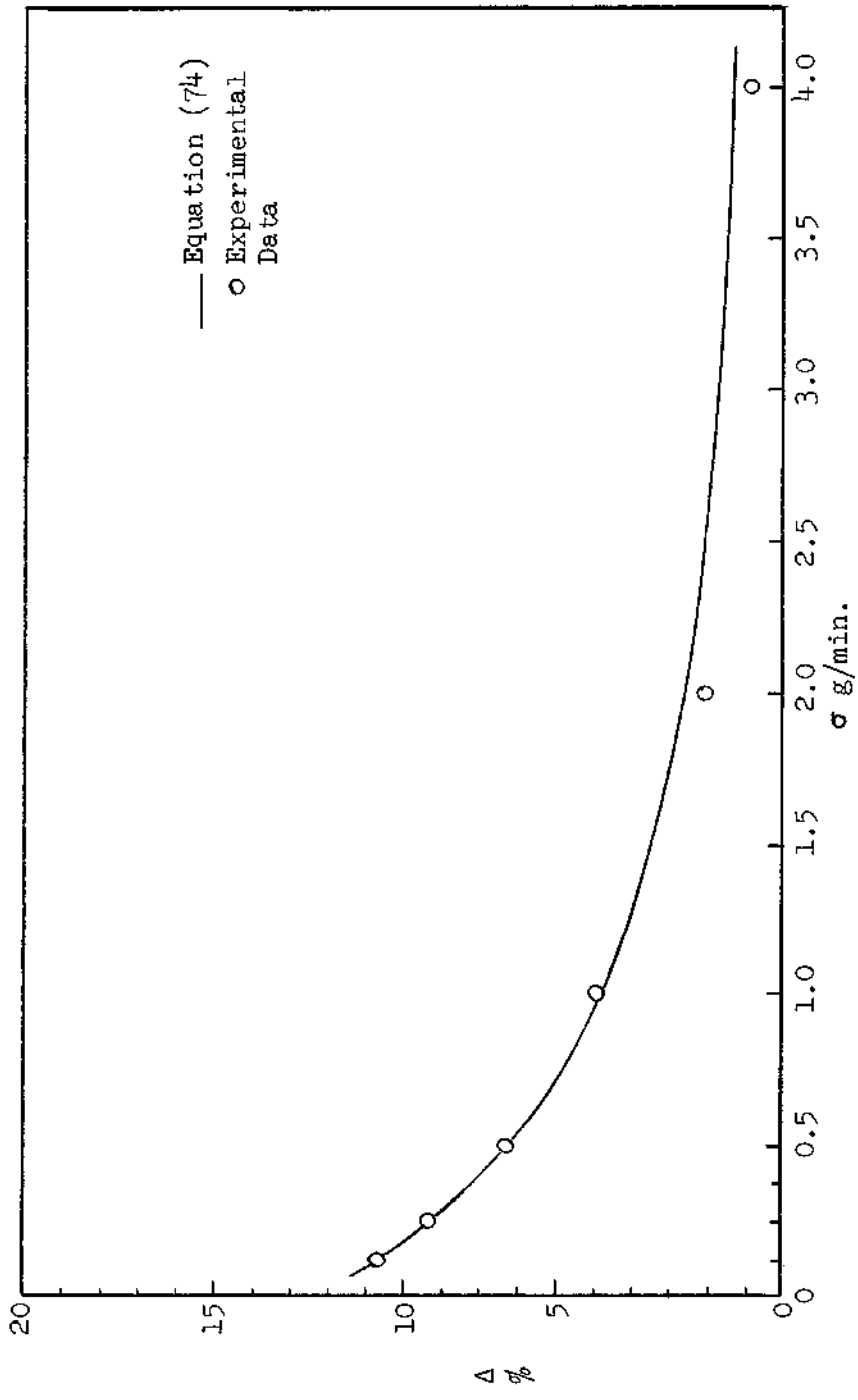

Figure 17. Degree of Separation of Toluene-Isobutyl Alcohol Azeotropic Mixture Versus Flow Rate at $\phi = 25^{0}$

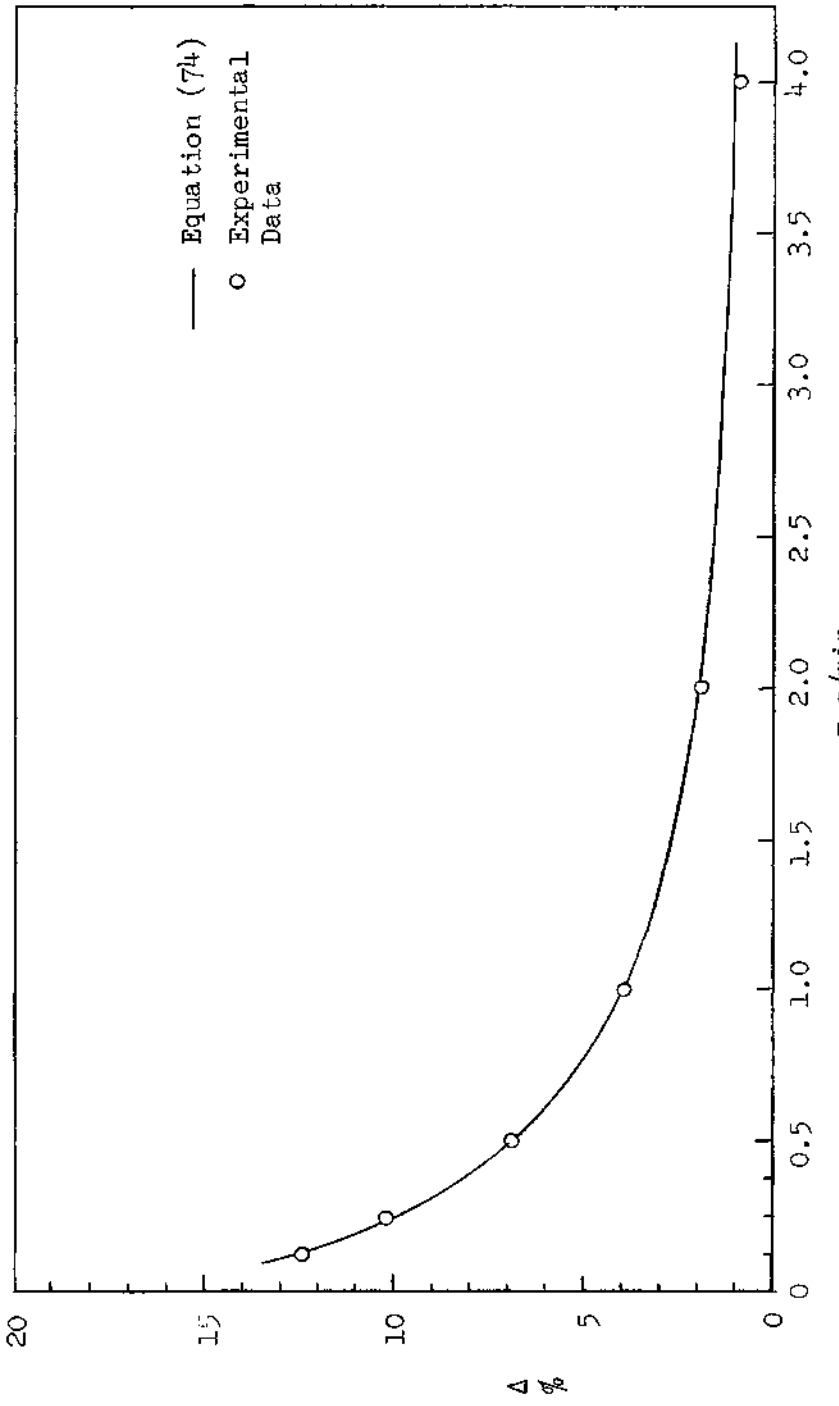

Figure 18. Degree of Separation of Toluene-Isobutyl Alcohol Azeotropic Mixture Versus Flow Rate at $\phi = 37^{0}$

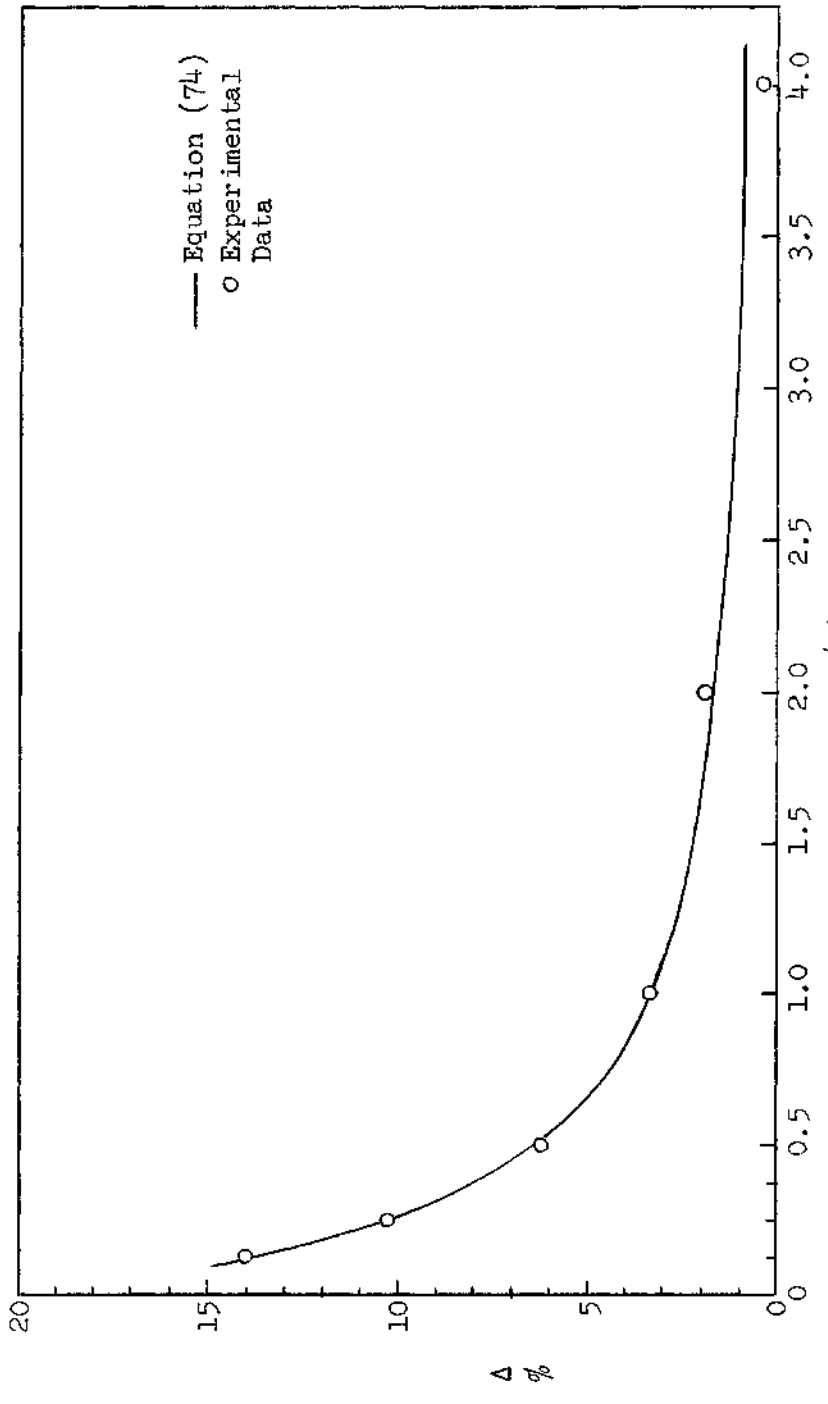

Figure 19. Degree of Separation of Toluene-Isobutyl Alcohol Azeotropic Mixture Versus Flow Rate at $\phi = 43^{\circ}$

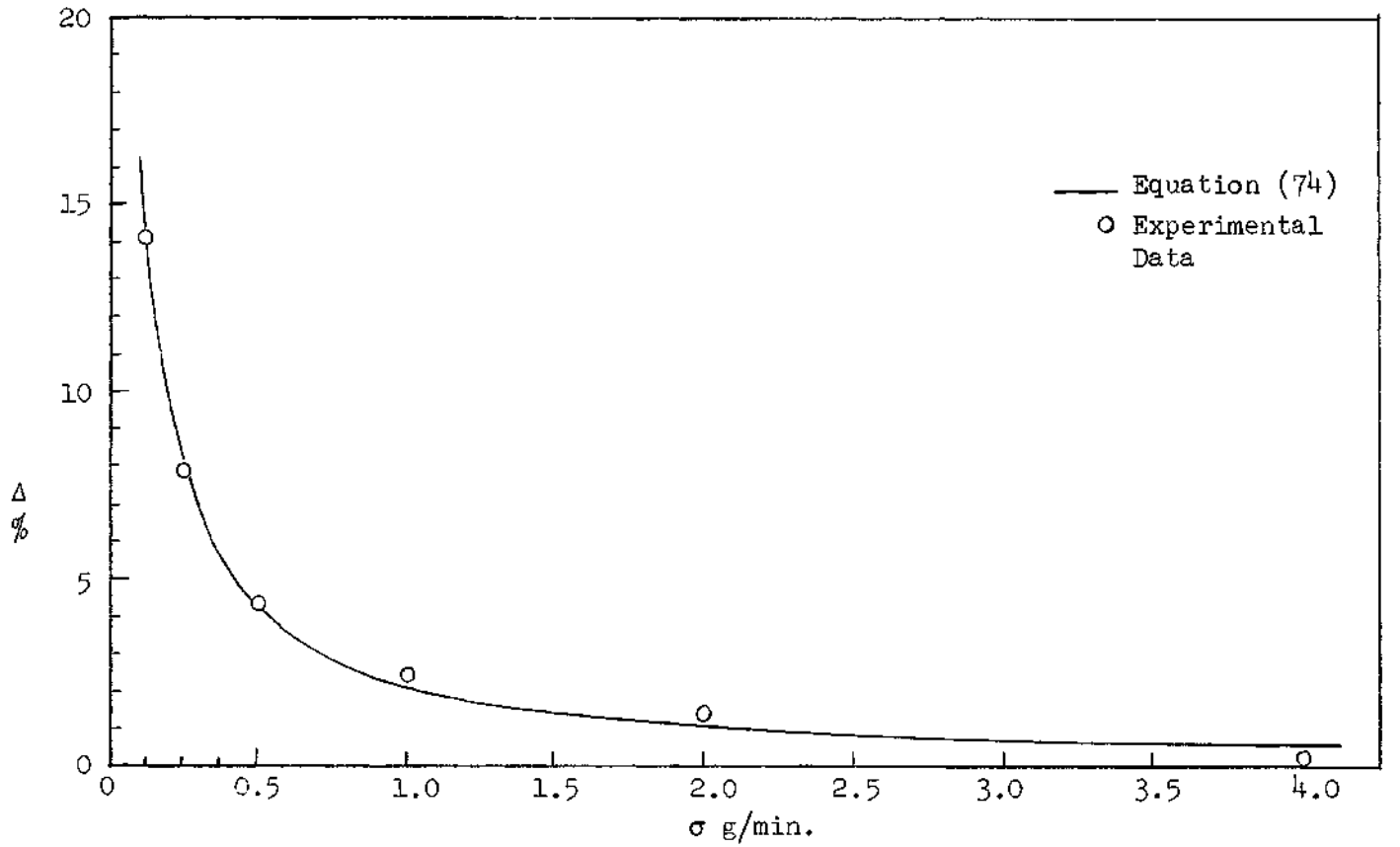

Figure 20. Degree of Separation of Toluene-Isobutyl Alcohol Azeotropic Mixture Versus Flow Rate at $\phi = 54^{o}$

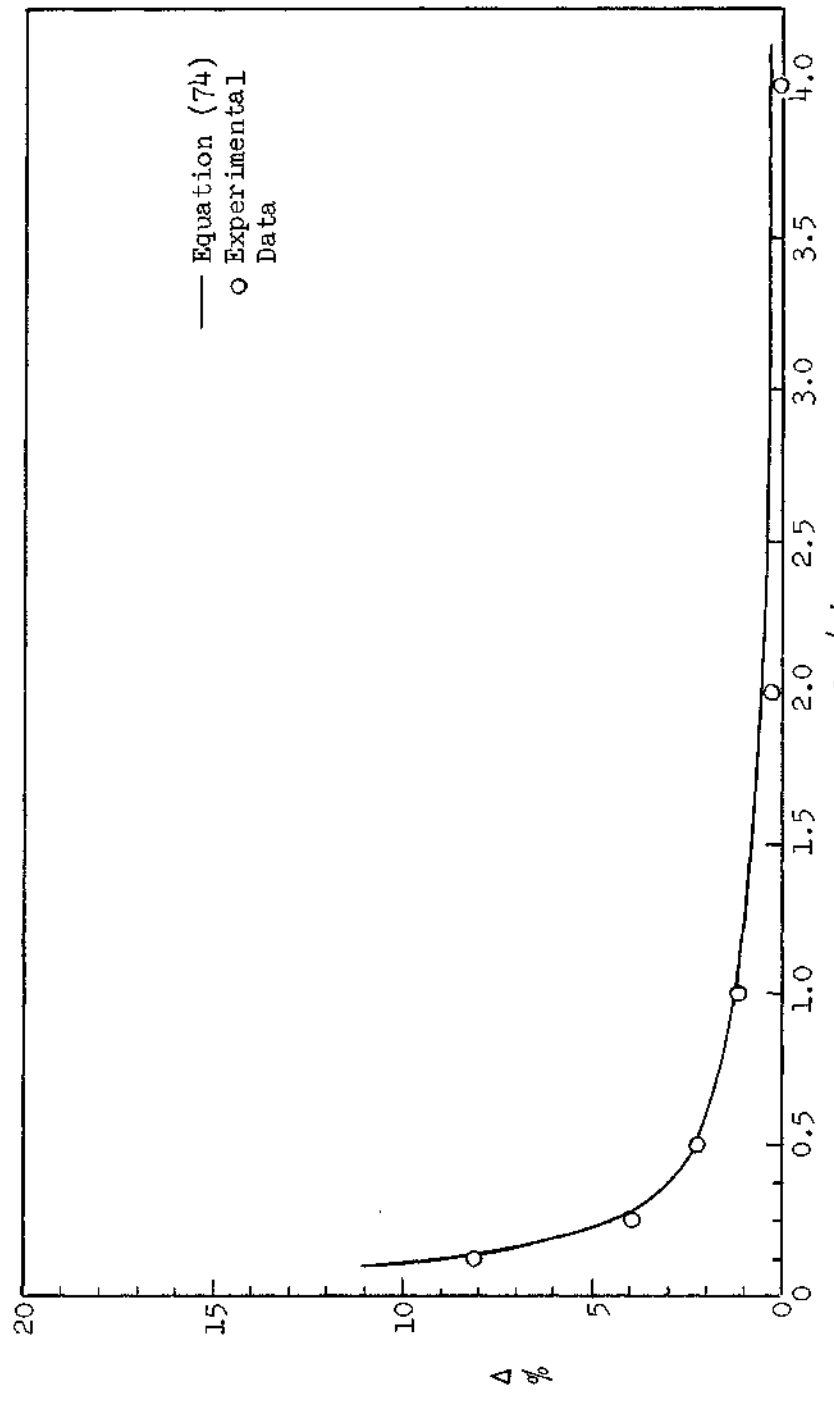

Figure 21. Degree of Separation of Toluene-Isobutyl Alcohol Azeotropic Mixture Versus Flow Rate at $\phi = 65^{0}$

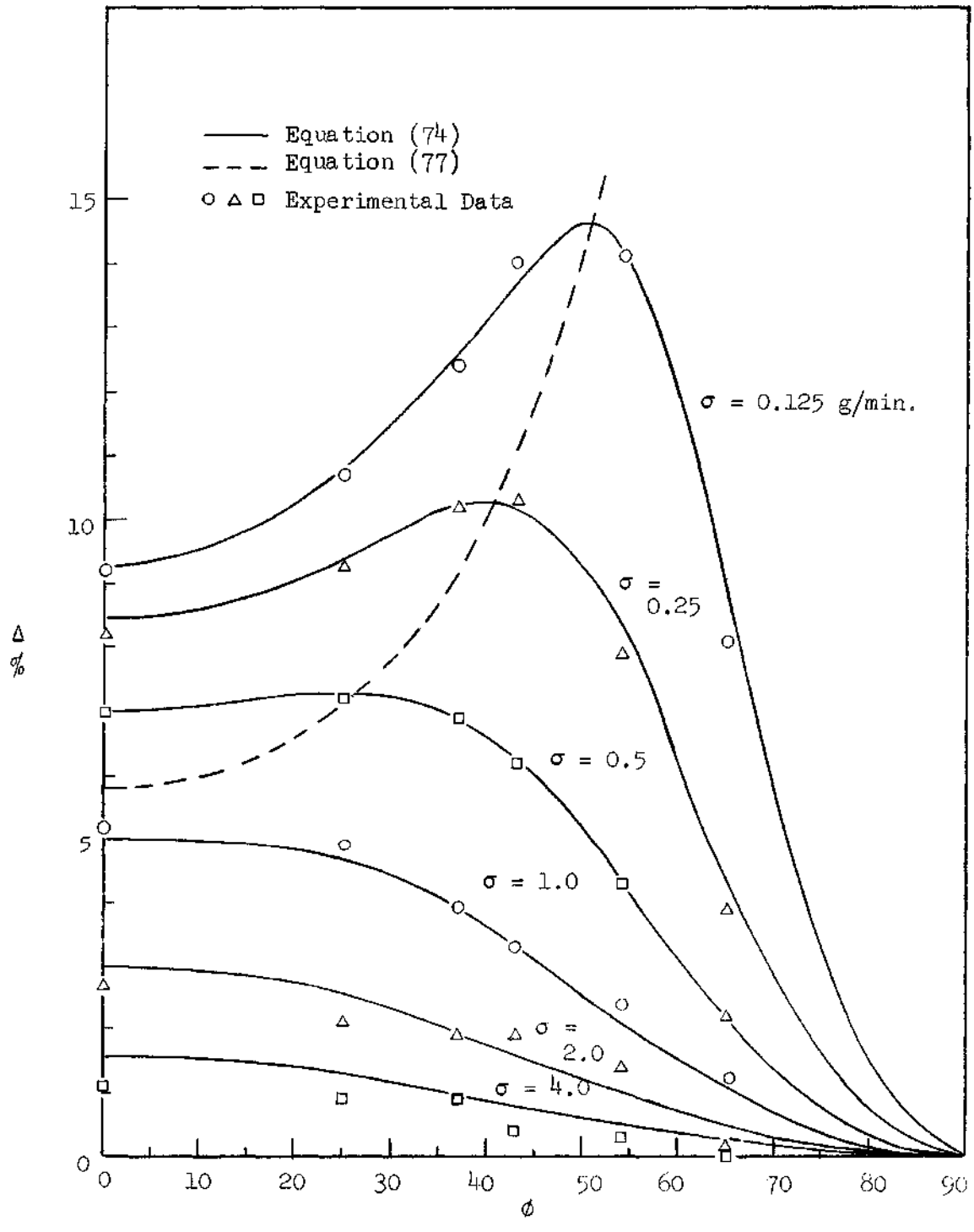

Figure 22. Effect of Wire Angle of Inclination on Degree of Separation of Toluene-Isobutyl Alcohol Azeotropic Mixture Obtained at Various Flow Rates

the column and operating conditions. This equation is plotted as solid lines in Figures 9 through 14. It can be seen that Equation (67), evaluated from the run with $\phi = 45.5^{o}$, will correlate other runs with different wire angles of inclinations.

The experimental data were replotted in Figure 15 using flow rate as a parameter to find out the effect of wire angle on the separation. The results indicate that maximum separations were obtained at optimum wire angles for the lower five flow rates.

Substitution of $H_o = 0.25$ and $K_o = 20.3$ into Equations (49) and (50) results in

$$\phi_{opt} = \cos^{-1} (0.809\ \sigma^{\frac{1}{11}}) \tag{68}$$

$$\Delta_{max} = 0.0585\ \sigma^{-\frac{1}{2}} \quad . \tag{69}$$

Combining Equations (68) and (69) gives

$$\Delta_{max} = \frac{0.0383}{\cos^{2}(\phi_{opt})} \quad . \tag{70}$$

Equation (70) is plotted in Figure 15 as a dotted line. Equations (68) and (69) are limited to the range of

$$0.027 < \sigma < 2.33 \text{ g/min} \quad . \tag{71}$$

A similar procedure was used to obtain the corresponding values and equations for the toluene-isobutyl alcohol azeotropic mixture. The experimental quantities are:

$$\sigma_A = 0.5 \text{ g/min} , \quad \Delta_A = 0.069 \text{ wt. fraction of toluene}$$

$$\sigma_B = 1.0 \text{ g/min} , \quad \Delta_B = 0.039 \text{ wt. fraction of toluene}$$

$$h = 22 \text{ in.}, \ \phi = 37 \text{ deg} , \ \Delta T = 80^\circ \text{ F.}$$

The corresponding results are

$$H_o = 0.125 \text{ g/min} \tag{72}$$

$$K_o = 6.66 \text{ g in./min} \tag{73}$$

$$\Delta = \frac{0.0625 \cos^2 \phi}{\sigma} \left(1 - e^{-\frac{1.65 \sigma}{\cos^4 \phi}} \right) \tag{74}$$

$$\phi_{opt} = \cos^{-1} (1.07 \sigma^{\frac{1}{4}}) \tag{75}$$

$$\Delta_{max} = 0.0513 \sigma^{-\frac{1}{2}} \tag{76}$$

$$\Delta_{max} = \frac{0.0587}{\cos^2(\phi_{opt})} \tag{77}$$

$$0.0165 < \sigma < 0.764 \quad . \tag{78}$$

Equation (74) is the separation equation for the toluene-isobutyl alcohol azeotropic mixture for all wire angles of inclination and all flow rates for the column and operating conditions. This equation is plotted as solid lines in Figures 16 through 21. The experimental data were replotted in Figure 22 using flow rate as a parameter to find out the effect of wire angle on the separation. The result indicates that

maximum separations were obtained at optimum wire angles for the three lower flow rates. Equation (77) is plotted in Figure 22 as a dotted line.

The improvement in separation by operating at the optimum wire angle is best illustrated by calculating the percentage increase in separation based on the open column (the column without a wire spiral). These results are presented in Tables 1 and 2.

Table 1. Comparison of Separation of An Equal Weight Fraction Mixture of Benzene-n-Heptane Obtained in An Open Column and a Wired Column Operating at Best Wire Angle of Inclination

σ g/min.	Δ_o %	$\Delta_{max.}$ %	$\phi_{opt.}$ deg.	Improvement $(\Delta_{max}-\Delta_o)/\Delta_o$ %
0.125	6.6	16.6	60.7	152
0.25	6.3	11.75	55	87
0.5	5.9	8.25	47	40
1.0	5.2	6.05	36	16
2.0	4.1	4.16	15.7	1.5

Table 2. Comparison of Separation of the Toluene-Isobutyl Alcohol Azeotropic Mixture Obtained in An Open Column and a Wired Column Operating at Best Wire Angle of Inclination

σ g/min.	Δ_o %	$\Delta_{max.}$ %	$\phi_{opt.}$ deg.	Improvement $(\Delta_{max}-\Delta_o)/\Delta_o$ %
0.125	9.3	14.6	50.5	57
0.25	8.4	10.3	40.7	22.6
0.5	7	7.3	25.8	4.3

CHAPTER VI

CONCLUSIONS AND RECOMMENDATIONS

Conclusions

On the basis of the results of this study, the following conclusions were reached.

1. It has been shown that the undesirable remixing effect in a concentric tube thermal diffusion column can be effectively reduced and a substantial increase in separation obtained by inserting in the annulus a tight fitting wire spiral having a diameter equal to the annular spacing and wrapped on the entire inner tube.

2. A generalized equation of separation, Equation (41), applicable to the cases: $\Delta < 0.4$, $\overline{cc} \cong 0.25$, and the annular spacing small compared with the tube diameter, has been derived.

3. A modified equation of separation, Equation (43), applicable only to moderate flow rates, was obtained from Equation (41). Operation under high flow rates, however, is very inefficient and therefore Equation (43) is the practical equation of separation for a real wired concentric tube thermal diffusion column.

4. The solutions for the best wire angle of inclination, Equation (49), and the maximum separation, Equation (50), have been obtained; further, the region within which the wire spiral improves the separation has been delineated. These results have been rewritten in dimensionless form and plotted in Figure 5.

5. Experimental results for the benzene-n-heptane and toluene-isobutyl alcohol systems quantitatively confirm the prediction of the theory, as shown in Figures 9 through 22.

Recommendations

It is suggested that further research in the following areas be conducted.

1. The improvement in separation of concentric tube thermal diffusion columns with either tube rotated.

2. A study of the efficiency of thermal diffusion fractionation in packed columns.

3. The improvement in separation of parallel plate thermal diffusion columns under linear fluid shear.

APPENDICES

APPENDIX A

EXPERIMENTAL DATA

Table 3. Experimental Data for Separation of the Benzene-n-Heptane System
$\Delta T = 75^{\circ}F$, Feed: 50 wt. % n-heptane

ϕ deg.	σ g/min.	Refractive Index (77°F) Top	Refractive Index (77°F) Bottom	Wt. Fraction of n-Heptane Top	Wt. Fraction of n-Heptane Bottom	Δ %
0	0.125	1.4268	1.4346	0.5295	0.4635	6.6
0	0.25	1.4269	1.4341	0.529	0.467	6.2
0	0.5	1.4270	1.4338	0.528	0.470	5.8
0	1.0	1.4271	1.4332	0.527	0.475	5.2
0	2.0	1.4282	1.4330	0.517	0.477	4.0
0	4.0	1.4284	1.4314	0.515	0.490	2.5
17.5	0.125	1.4260	1.4345	0.537	0.464	7.3
17.5	0.25	1.4262	1.4343	0.535	0.466	6.9
17.5	0.5	1.4267	1.4342	0.530	0.4665	6.35
17.5	1.0	1.4267	1.4329	0.530	0.478	5.2
17.5	2.0	1.4273	1.4324	0.525	0.482	4.3
17.5	4.0	1.4284	1.4314	0.515	0.490	2.5
32	0.125	1.4255	1.4358	0.542	0.454	8.8
32	0.25	1.4256	1.4353	0.541	0.458	8.3
32	0.5	1.4260	1.4348	0.537	0.462	7.5
32	1.0	1.4264	1.4334	0.533	0.473	6.0
32	2.0	1.4275	1.4325	0.522	0.481	4.1
32	4.0	1.4286	1.4315	0.514	0.489	2.5
45.5	0.125	1.4239	1.4380	0.558	0.435	12.3
45.5	0.25	1.4247	1.4370	0.550	0.444	10.6
45.5	0.5	1.4255	1.4350	0.542	0.460	8.2
45.5	1.0	1.4270	1.4336	0.5275	0.472	5.45
45.5	2.0	1.4286	1.4321	0.514	0.484	3.0
45.5	4.0	1.4295	1.4314	0.506	0.490	1.6

(continued)

Table 3. (Continued)

ϕ deg.	σ g/min.	Refractive Index (77°F) Top	Refractive Index (77°F) Bottom	Wt. Fraction of n-Heptane Top	Wt. Fraction of n-Heptane Bottom	Δ %
58	0.125	1.4220	1.4402	0.577	0.417	16.0
58	0.25	1.4241	1.4373	0.556	0.441	11.5
58	0.5	1.4259	1.4345	0.538	0.464	7.4
58	1.0	1.4277	1.4331	0.521	0.476	4.5
58	2.0	1.4293	1.4313	0.508	0.491	1.7
58	4.0	1.4297	1.4306	0.504	0.497	0.7
70	0.125	1.4246	1.4373	0.551	0.441	11.0
70	0.25	1.4270	1.4330	0.528	0.477	5.1
70	0.5	1.4286	1.4321	0.514	0.484	3.0
70	1.0	1.4295	1.4311	0.506	0.492	1.4
70	2.0	1.4297	1.4304	0.504	0.498	0.6
70	4.0	1.4302	1.4302	0.500	0.500	0.0

Table 4. Experimental Data for Separation of the Toluene-Isobutyl Alcohol System
$\Delta T = 80^{\circ}F$, Feed: 55.42 wt. % Toluene (Azeotropic Composition)

ϕ deg.	σ g/min.	Refractive Index ($80^{\circ}F$) Top	Bottom	Wt. Fraction of Toluene Top	Bottom	Δ %
0	0.125	1.4491	1.4393	0.599	0.507	9.2
0	0.25	1.4488	1.4405	0.596	0.514	8.2
0	0.5	1.4481	1.4410	0.589	0.519	7.0
0	1.0	1.4472	1.4420	0.581	0.529	5.2
0	2.0	1.4458	1.4431	0.567	0.540	2.7
0	4.0	1.4451	1.4440	0.5605	0.5495	1.1
25	0.125	1.4497	1.4390	0.606	0.499	10.7
25	0.25	1.4492	1.4400	0.601	0.508	9.3
25	0.5	1.4485	1.4412	0.593	0.521	7.2
25	1.0	1.4470	1.4421	0.579	0.530	4.9
25	2.0	1.4456	1.4434	0.565	0.544	2.1
25	4.0	1.4449	1.4439	0.558	0.549	0.9
37	0.125	1.4510	1.4385	0.618	0.494	12.4
37	0.25	1.4498	1.4395	0.606	0.504	10.2
37	0.5	1.4479	1.4411	0.588	0.519	6.9
37	1.0	1.4465	1.4426	0.574	0.535	3.9
37	2.0	1.4455	1.4435	0.564	0.545	1.9
37	4.0	1.4450	1.4441	0.5595	0.5505	0.9
43	0.125	1.4516	1.4375	0.624	0.484	14.0
43	0.25	1.4495	1.4391	0.603	0.500	10.3
43	0.5	1.4477	1.4415	0.586	0.524	6.2
43	1.0	1.4462	1.4430	0.572	0.539	3.3
43	2.0	1.4455	1.4435	0.564	0.545	1.9
43	4.0	1.4446	1.4442	0.5555	0.5515	0.4

(continued)

Table 4. (Continued)

ϕ deg.	σ g/min.	Refractive Index (80°F) Top	Bottom	Wt. Fraction of Toluene Top	Bottom	Δ %
54	0.125	1.4516	1.4374	0.624	0.483	14.1
54	0.25	1.4485	1.4406	0.594	0.515	7.9
54	0.5	1.4470	1.4426	0.579	0.535	4.4
54	1.0	1.4457	1.4433	0.566	0.542	2.4
54	2.0	1.4453	1.4439	0.562	0.548	1.4
54	4.0	1.4447	1.4444	0.5565	0.5535	0.3
65	0.125	1.4486	1.4404	0.594	0.513	8.1
65	0.25	1.4469	1.4430	0.578	0.539	3.9
65	0.5	1.4458	1.4436	0.567	0.545	2.2
65	1.0	1.4453	1.4440	0.562	0.550	1.2
65	2.0	1.4446	1.4444	0.555	0.553	0.2
65	4.0	1.4445	1.4445	0.5542	0.5542	0.0

APPENDIX B

CALIBRATION CURVES

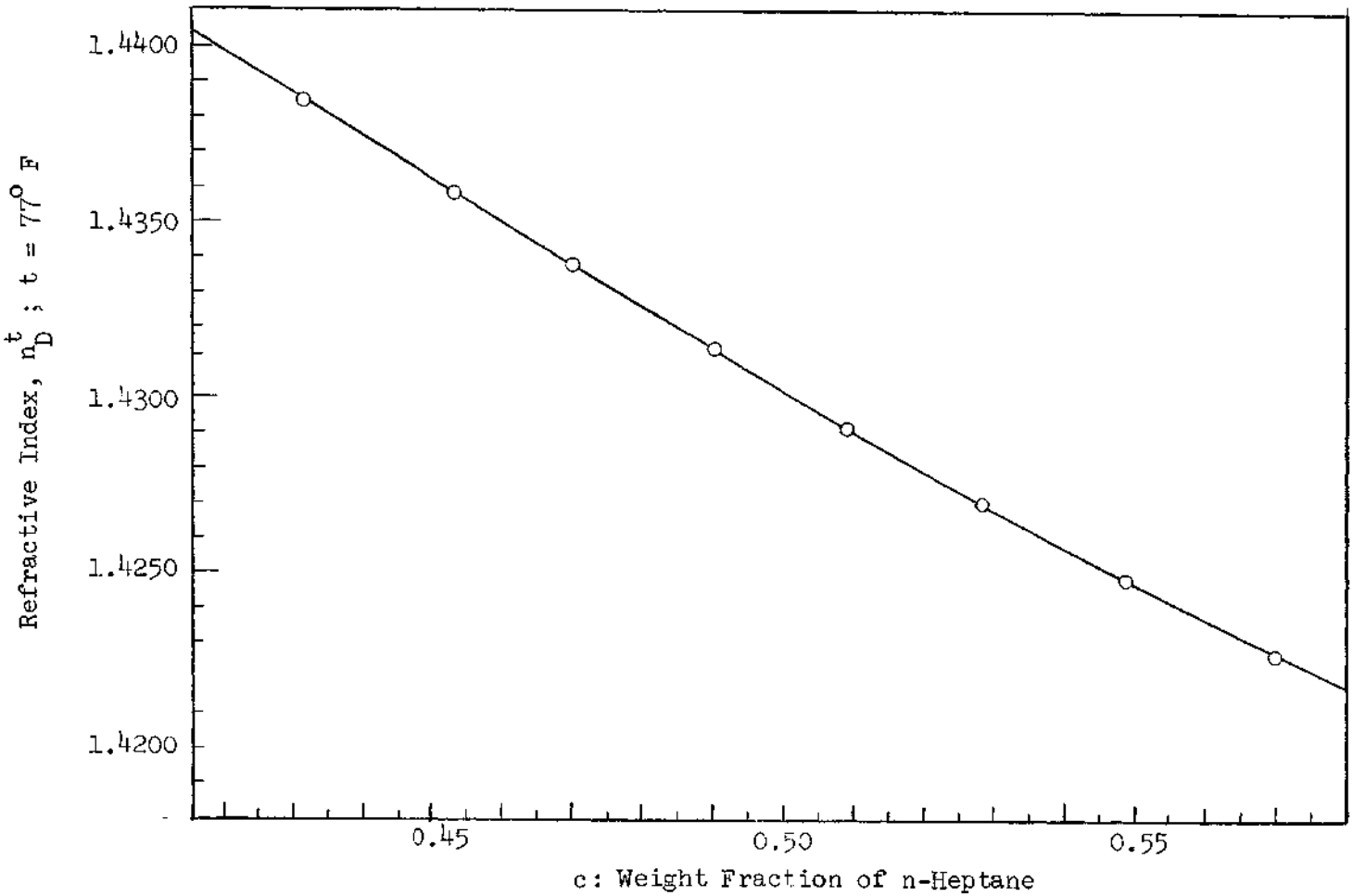

Figure 23. Refractive Index of Benzene-n-Heptane System at 77° F

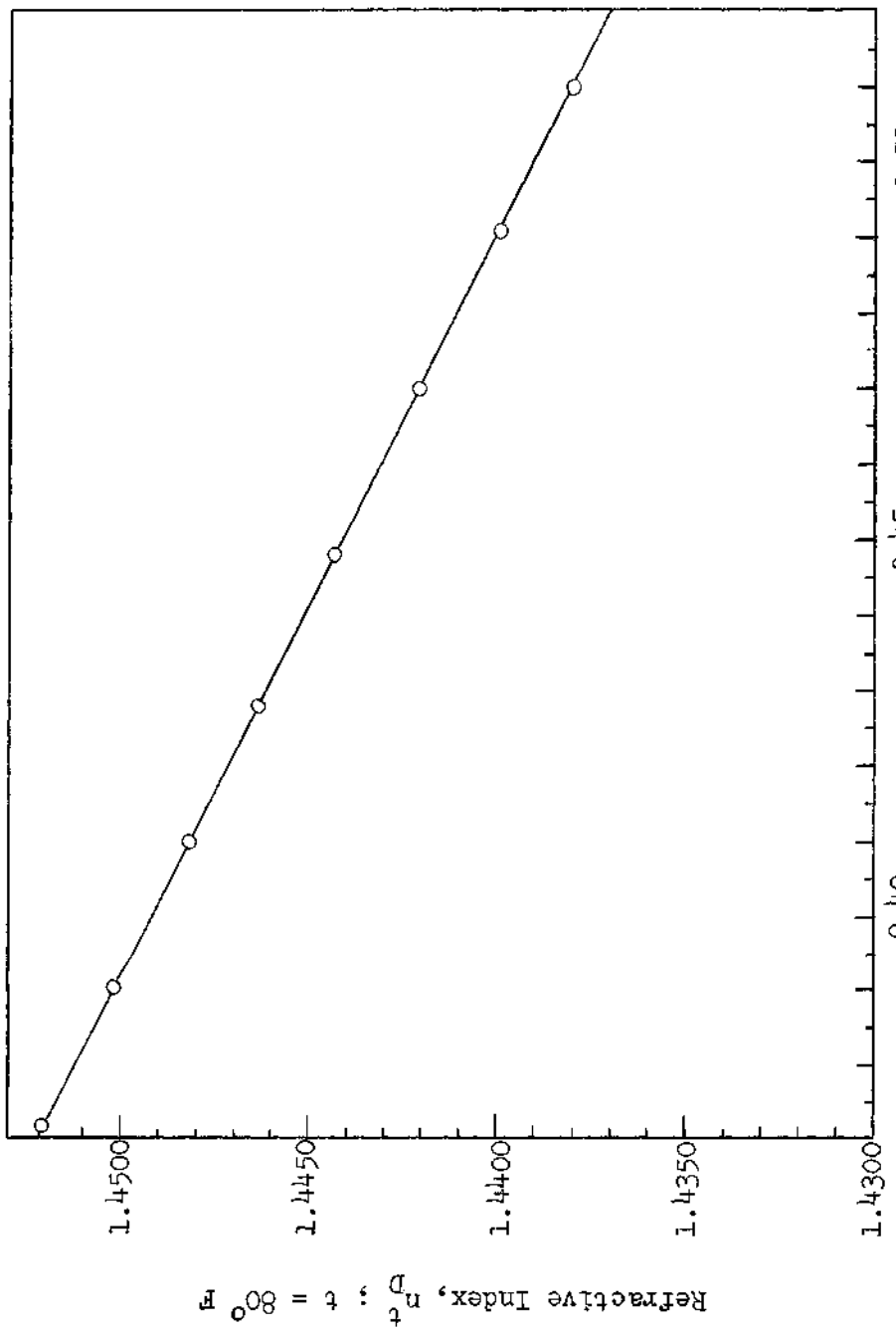

Figure 24. Refractive Index of Toluene-Isobutyl Alcohol System at 80° F

BIBLIOGRAPHY

1. Chapman, S. and Dootson, F. W., "A Note on Thermal Diffusion," Philosophical Magazine and Journal of Science, Vol. 33, 1917.

2. Chueh, P. L. and Yeh, H. M., "Thermal Diffusion in a Flat-Plate Column Inclined for Improved Performance," American Institute of Chemical Engineering Journal, Vol. 13, No. 1, 1967.

3. Clusius, K. and Dickel, G., "Neues Verfahren zur Gasentmischung und Isotopentrennung," Die Naturwissenschaften, Vol. 26, 1938.

4. Clusius, K. and Dickel, G., "Das Trennrohr," Zeitschrift fer Physikalische Chemie, Part B, Vol. 44, 1939.

5. Cuming, H. G., "The Secondary Flow in Curved Pipe," Great Britain Aeronautical Research Council, Reports and Memoranda, No. 2880.

6. Debye, P. and Bueche, A. M., High Polymer Physics, A Symposium, H. A. Robinson, ed., Chemical Publishing Company, Brookly, New York, 1948.

7. Enskog, D., "Uber eine Verallgemeinerung der zweiten Maxwellschen Theorie der Gase," and "Bermerkungen zu einer Fundamentaleichung in der Kinetischen Gastheroie," Physikalische Zeitschrift, Vol. 12, 1911.

8. Dufour, L., Archives des Sciences Physiques et Naturelles, Vol. 45, 1872, pp. 9-12.

9. Furry, W. H., Jones, R. H., and Onsager, L., "On the Theory of Isotope Separation by Thermal Diffusion," Physical Review, Vol. 55, 1939.

10. Jones, R., Clark, and Furry, W. H., "The Separation of Isotopes by Thermal Diffusion," Reviews of Modern Physics, Vol. 18, 1946.

11. Powers, J. E. and Wilke, C. R., "Separation of Liquids by Thermal Diffusion," American Institute of Chemical Engineering Journal, Vol. 3, 1957.

12. Sullivan, L. J., Ruppel, T. C., and Willingham, C. B., "Rotary and Packed Thermal Diffusion Fractionating Columns for Liquids," Industrial and Engineering Chemistry, Vol. 47, 1955.

13. Sullivan, L. J., Ruppel, T. C., and Willingham, C. B., "Packed Thermal Diffusion Column," Industrial and Engineering Chemistry, Vol. 49, 1957.

14. Washall, T. A. and Melpolder, F. W., "Improving the Separation Efficiency of Liquid Thermal Diffusion Column," Industrial and Engineering Chemistry, Process Design and Development, Vol. 1, No. 1, 1962.

VITA

Ho-Ming Yeh was born in Taiwan, China on January 28, 1937. He attended the Shen-Li Elementary School and the Chang-Jung High School in Tainan, Taiwan.

He entered the National Taiwan University in Taipei, Taiwan and received the degree of Bachelor of Chemical Engineering in June, 1960. After he had received the degree of Master of Science in Chemical Engineering at Cheng Kung University in June, 1964 in Tainan, Taiwan, he was employed as an instructor by the Department of Chemical Engineering of Cheng Kung University and was promoted to Associate Professor in August, 1968.

In September, 1967 he received a fellowship from the Chinese National Science Council for graduate studies leading to the Ph.D. degree at the Georgia Institute of Technology in the School of Chemical Engineering.

He is married to the former Mei-Huey Lee of Tainan, Taiwan and they have two children.